Turner et al. BMC Biology 2014, 12:63
http://www.biomedcentral.com/1741-7007/12/63

BMC Biology

RESEARCH ARTICLE Open Access

Brachyury cooperates with Wnt/β-catenin signalling to elicit primitive-streak-like behaviour in differentiating mouse embryonic stem cells

David A Turner*, Pau Rué, Jonathan P Mackenzie, Eleanor Davies and Alfonso Martinez Arias*

Abstract

Background: The formation of the primitive streak is the first visible sign of gastrulation, the process by which the three germ layers are formed from a single epithelium during early development. Embryonic stem cells (ESCs) provide a good system for understanding the molecular and cellular events associated with these processes. Previous work, both in embryos and in culture, has shown how converging signals from both nodal/TGFβR and Wnt/β-catenin signalling pathways specify cells to adopt a primitive-streak-like fate and direct them to undertake an epithelial-to-mesenchymal transition (EMT). However, many of these approaches have relied on genetic analyses without taking into account the temporal progression of events within single cells. In addition, it is still unclear to what extent events in the embryo are able to be reproduced in culture.

Results: Here, we combine flow cytometry and a quantitative live single-cell imaging approach to demonstrate how the controlled differentiation of mouse ESCs towards a primitive streak fate in culture results in cells displaying many of the characteristics observed during early mouse development including transient brachyury expression, EMT and increased motility. We also find that the EMT initiates the process, and this is both fuelled and terminated by the action of brachyury, whose expression is dependent on the EMT and β-catenin activity.

Conclusions: As a consequence of our analysis, we propose that a major output of brachyury expression is in controlling the velocity of the cells that are transiting out of the primitive streak.

Keywords: Wnt, β-catenin, mouse embryonic stem cell, mesendoderm, primitive streak, live-cell imaging, brachyury, epithelial-to-mesenchymal transition, EMT, activin, nodal

Background

The development of an organism is the result of the proliferation, concomitant phenotypic diversification and spatial organization of cells in the context of spatiotemporally controlled patterns of gene expression [1-3]. The use of genetics to interrogate these processes has revealed that they are underpinned by the temporal iteration of coordinated interactions between signal transduction and transcription factor networks. Establishing the relationship between these molecular events and the emergence of cellular diversity is an essential step towards understanding the relationship between programs of gene activity and the process of morphogenesis that shapes cells into tissues and organs.

Gastrulation is one of the earliest events where it is possible to observe a convergence of fate specification and morphogenetic processes in embryos [1]. It occurs in all metazoans and encompasses a choreography of cell movements that transforms a group of seemingly identical epithelial cells, with species-specific geometry, into the outline of an organism exhibiting an overt anterior-posterior organization and three germ layers (ectoderm, mesoderm and endoderm) [4-6]. In chordates, gastrulation is led by a dynamic population of cells that gives rise to the mesoderm and the endoderm, defines and patterns the neuroectoderm and delineates the plane of bilateral symmetry [6,7]. In mammalian embryos this population, called the primitive streak, is associated with the expression of the T-box transcription factor brachyury (Bra) [4,8-11]. In the mouse, Bra is first expressed shortly after implantation in a group of cells at the

* Correspondence: dat40@cam.ac.uk; ama11@hermes.cam.ac.uk
Department of Genetics, University of Cambridge, Cambridge CB2 3EH, UK

BioMed Central

© 2014 Turner et al.; licensee BioMed Central Ltd. This is an Open Access article distributed under the terms of the Creative Commons Attribution License (http://creativecommons.org/licenses/by/4.0), which permits unrestricted use, distribution, and reproduction in any medium, provided the original work is properly credited. The Creative Commons Public Domain Dedication waiver (http://creativecommons.org/publicdomain/zero/1.0/) applies to the data made available in this article, unless otherwise stated.

boundary between the prospective embryonic and extra-embryonic tissues. At stage E6.5, preceding the onset of gastrulation movements, Bra expression becomes restricted to the proximal posterior region of the embryo [9], at the position where under the influence of nodal and Wnt signalling, the primitive streak is initiated as a dynamic structure that will progress towards the distal end of the epiblast, ploughing an anteroposterior axis [12]. At the cellular level, gastrulation involves a sequence of highly organized epithelial-to-mesenchymal transition (EMT) movements that propagate through the tissue in a manner that resembles a travelling wave [13-15]. The first cells undergoing EMT ingress and move towards the anterior contralateral side of the embryo. This movement accompanies the distal/anterior spread of the streak and thus, by the end of gastrulation, two-thirds of the epiblast has been wrapped by the cells that have undergone gastrulation. This choreography of cell movements is characterized by the expression of a number of transcription factors at the leading edge of the EMT, in particular brachyury [11], Eomes [16] and Mixl1 [17].

Just anterior to the primitive streak there is a structure, the organizer, which does not undergo an EMT, shows homology with the Spemann organizer and will become the node when the streak reaches the distal-most anterior region of the epiblast at about E7.5 [18]. The organizer and the node express Bra and after E7.5 the node regresses towards the posterior pole of the embryo, leaving the notochord in its wake. The node and the notochord continue to express Bra. After this time, Bra expression becomes restricted to a region in the tail that will undergo caudal extension to generate the caudal spinal cord and somatic mesoderm, [6,10,19-21]. Genetic analysis has shown that in embryos, Bra is required for both movement of the cells through the primitive streak during axial extension and their specification into the mesoderm and notochord posterior to somite 7 [22-24].

The localization of Bra expression to the proximal posterior region of the epiblast is a useful reference for the onset of gastrulation. Genetic analysis has identified a requirement for bone morphogenetic factor (BMP), Wnt/β-catenin and nodal for this event [25]. These studies have also shown that BMP sets up the expression of nodal and Wnt3a, which, from the visceral endoderm, are likely to be the direct activators of Bra expression. How individual cells integrate nodal and Wnt signalling with the expression of Bra to promote the directional EMT and how these events are coordinated across the cell population that is defined as the primitive streak is not known. While there are some reports of the gastrulation movements in mouse embryos with a cellular resolution [15,26], these are descriptive and the visualization systems do not lend themselves to experimental perturbations.

Embryonic stem cells (ESCs), clonal populations of cells from the pre-implantation blastocysts [27,28], can be differentiated in culture into Bra-expressing cells that exhibit gene expression profiles characteristic of the primitive streak [8,29-36]. In addition to gene expression analysis, ESCs also offer the opportunity to quantify proteins at the level of single cells through live imaging. For these reasons, ESCs could provide a useful model for understanding the link between signals and morphogenesis in the context of the onset of gastrulation. However, to do this it is important to show that, in addition to patterns of gene expression, the differentiating ESCs share other features with the cells in the primitive streak, in particular EMT and its relationship to Bra expression.

Here we have used a combination of live-cell imaging, immunocytochemistry and chemical genetics to analyse the onset and consequences of Bra expression in mouse ESCs (mESCs) at the level of single cells. We observe that mESCs grown on gelatin and in the presence of activin (Act) and chiron (Chi, an agonist of Wnt/β-catenin signalling), undergo an EMT associated with the expression of Bra and that the EMT itself contributes to Bra expression. We are able to separate the inputs of β-catenin and Act into the onset of Bra expression and show that while β-catenin is required for the up-regulation of Bra, Act is required for the velocity, and thereby the distance cells travel. We discuss our findings in the context of the emergence of the primitive streak during gastrulation and suggest that differentiation of ESCs into Bra-expressing cells in culture provides a valuable system for studying the mechanisms that specify the emergence of the primitive streak.

Results

The onset of brachyury expression in culture

To probe the connection between the differentiation of mESCs and the onset of Bra expression in the embryo, we used a mESC line bearing an insertion of GFP into the Bra locus (Bra::GFP), which has been shown to display, upon differentiation, characteristics associated with the primitive streak during development [8,34]. We confirmed that this line faithfully reports the onset of Bra expression in culture by following, through fluorescence-activated cell sorting (FACS) analysis, Bra::GFP expression in a variety of differentiation conditions (Figure 1A) and comparing its expression profile to that of endogenous Bra protein and mRNA (Figure 1C). When Bra::GFP-expressing cells are grown in neural differentiation conditions, there is no GFP expression (Additional file 1: Figure S1) but growth in the presence of activin A (Act) and an inhibitor of GSK3, CHIR99021 (Chi, which mimics Wnt/β-catenin signalling), leads to a wave of Bra expression (Figure 1A) that parallels Bra mRNA and protein (Figure 1B,C). As this cell line is heterozygous for Bra, it is likely to exhibit an haploinsufficient phenotype associated with the Bra locus [20,37,38], but this

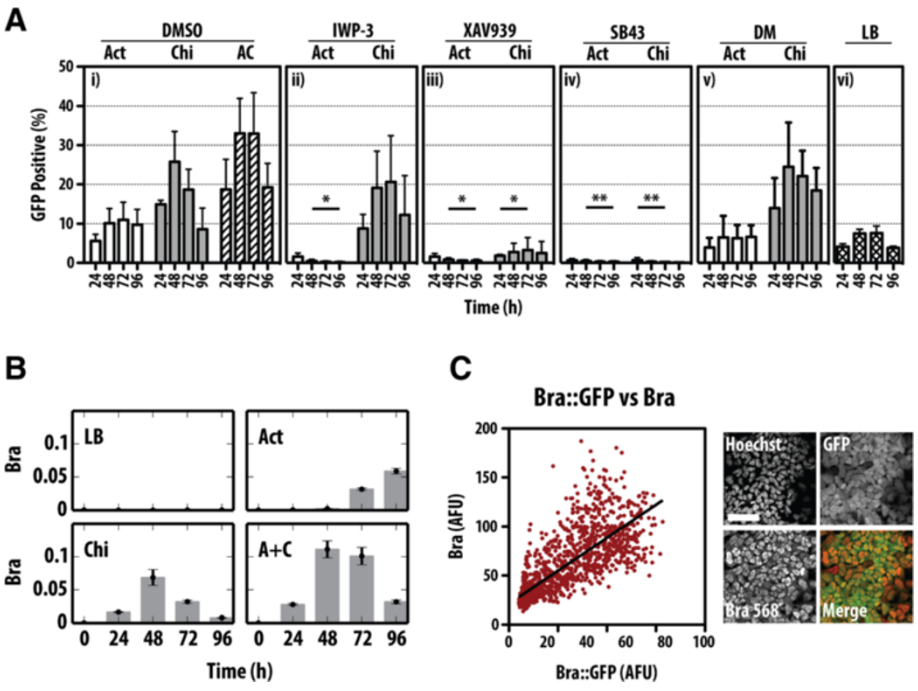

Figure 1 Induction of Bra expression by activin (Act) and CHIR99021 (Chi) during the differentiation of mESCs. (A) Bra::GFP mESCs were treated with Act, Chi or Act/Chi and dimethyl sulfoxide (DMSO) (i), Act and Chi with the Porcupine inhibitor IWP3, which inhibits the secretion of Wnt proteins (ii), with the tankyrase inhibitor XAV939, which reduces active β-catenin (iii), the nodal/Act receptor inhibitor SB431542 (SB43) (iv) or the BMP inhibitor dorsomorphin (v). A control for long-term pluripotency growth, leukaemia inhibitory factor (LIF) and BMP (LB), is included (vi). Notice that the robust expression of Bra induced by Act and Chi, is suppressed by inhibition of Wnt/β-catenin or nodal/Act signalling but not by BMP inhibition. Measurements were made with GFP-positive cells daily by FACS (±standard deviation from at least three replicates). Single and double asterisks denote $P < 0.05$ and $P < 0.01$, respectively, versus DMSO. **(B)** E14-Tg2A mESCs were grown in LB, Act, Chi or Act/Chi for the indicated durations prior to RNA extraction and quantitative real-time reverse-transcription-polymerase chain reaction (RT-qPCR) analysis for the indicated genes. The average expression level of the RT-qPCR replicates relative to that of glyceraldehyde 3-phosphate dehydrogenase (GAPDH) are shown for a representative experimental replicate. Error bars indicate absolute error of the normalized mean. Notice the transient expression of Bra in Chi and dual Act and Chi compared with the delayed expression in Act. **(C)** Quantification of Bra::GFP v Bra expression by immunostaining indicates a high correlation (Pearson coefficient of 0.773). Scale bar denotes 50 μm. A + C or AC, activin A + chiron; Act, activin A; AFU, arbitrary fluorescence units; Bra, brachyury; Chi, chiron CHIR99021; DM, dorsomorphin; DMSO, dimethyl sulfoxide; FACS, fluorescence-activated cell sorting; GAPDH, glyceraldehyde 3-phosphate dehydrogenase; GFP, green fluorescent protein; LB, leukaemia inhibitory factor and bone morphogenetic factor; RT-qPCR, quantitative real-time reverse-transcription-polymerase chain reaction.

should not interfere with the initiation of expression, which is the object of our study.

Individual treatment of the Bra::GFP mESCs with either Act (100 ng/ml) or Chi (3 μM) resulted in a transient rise in the proportion of cells expressing GFP (Figure 1A). For Act alone, we observe a peak of approximately 10% at 72 h, whereas treatment with Chi anticipates this peak with 25% of the total population expressing Bra::GFP at 48 h. The combination of Act and Chi (Act/Chi) results in an increase in the proportion of cells expressing Bra::GFP (approximately 33% GFP positive at 48 to 72 h), which is sustained relative to Chi alone. These observations extend previous ones [34,35] and suggest that both Act and Wnt/β-catenin signalling can influence the progression of pluripotent cells towards a state characterized by the expression of Bra.

To understand the individual contributions of Act and Wnt/β-catenin signalling to the expression of Bra::GFP, specific inhibitors targeting each pathway were added to the cell culture medium (Figure 1A). Inhibition of β-catenin signalling during Act treatment resulted in complete ablation of Bra::GFP induction compared with the DMSO control ($P < 0.05$). A similar effect was observed upon inhibition of Act signalling by SB43 (an inhibitor of Act/nodal signalling) in the presence of Act or Chi.

Taken together, these results are in agreement with previous observations [34] that the onset of Bra::GFP by Act ligands not only requires active β-catenin signalling, but that an active Act pathway is absolutely required for β-catenin-mediated Bra induction.

An epithelial-to-mesenchymal transition associated with mesendodermal differentiation in embryonic stem cells

In the embryo, the onset of Bra expression is associated with spatiotemporally organized cellular movements that configure the process of gastrulation [13,39]. To assess whether this behaviour was also observed in mESCs in these conditions, we analysed the cellular activities associated with Bra

expression in the adherent cultures by filming the behaviour of the cells in the presence of Act/Chi (Figure 2A), a condition that promotes the maximal Bra expression response (Figure 1A). We observe that after 24 h, the colonies characteristic of the pluripotent state loosen up and the differentiating cells form an epithelial monolayer from which they adopt a mesenchymal-like morphology and become motile (Figure 2A). This state is probably akin to the post-implantation epiblast and it is in this state that it is possible to observe the onset of

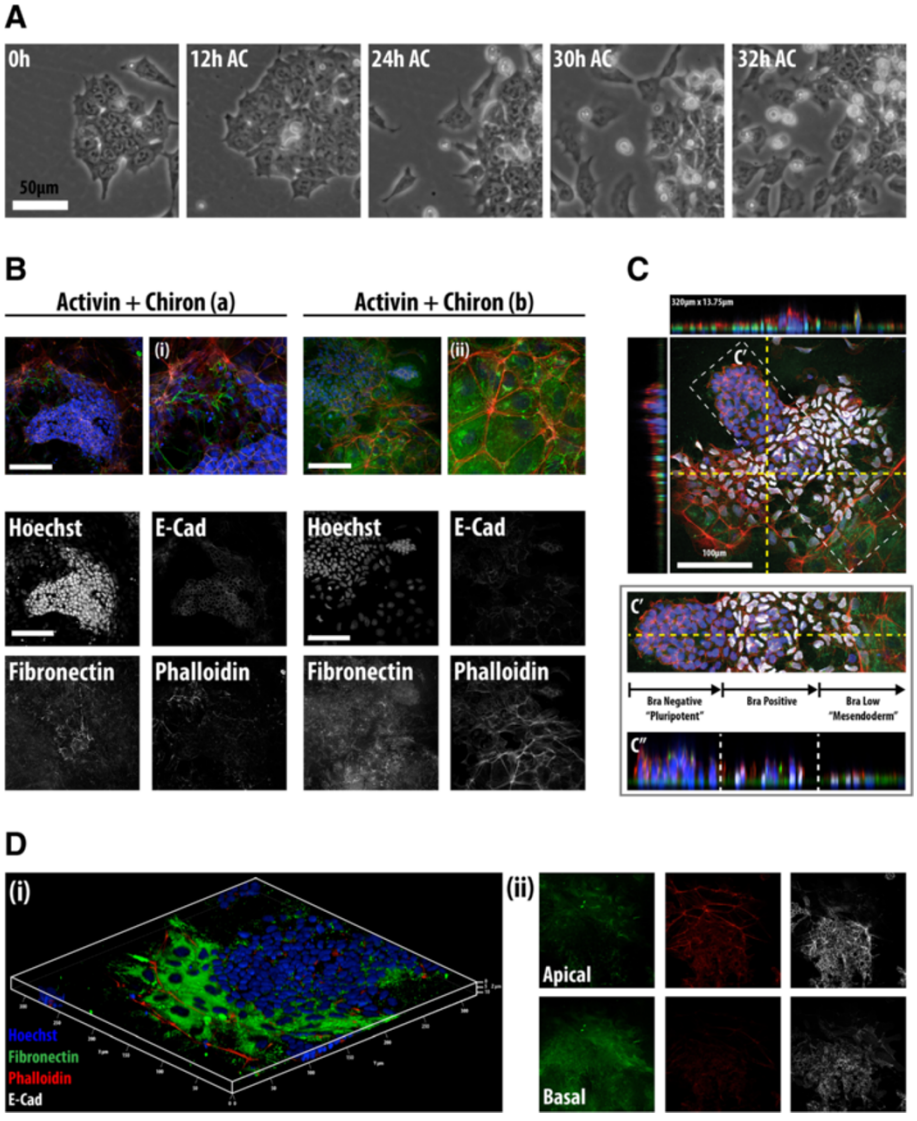

Figure 2 An EMT is associated with mesendodermal differentiation of E14-Tg2A. (A) Phase-contrast images from live-cell imaging of wild-type (WT) mESCs following Act/Chi. At the start of differentiation, cells begin to loosen up within the colonies, adopt a more motile morphology and become migratory over time. **(B,C)** Differentiating mESCs were treated with Act/Chi and stained for E-cadherin **(B)** or brachyury (**C** and Additional file 2: Figure S2D) together with fibronectin and phalloidin. Panels (a) and (b) in **(B)** show two separate colonies and their corresponding magnified regions (i and ii) in different phases of an EMT. The decrease in E-cadherin correlates with the appearance of filopodia and the laying down of fibronectin basally. This is clear at the edge of the colony, where these changes are associated with Bra expression (**C** and Additional file 2: Figure S2C); 320x13.75 μm sections through the colony, indicated by yellow hashed lines illustrate this (**C**, top). A region of the colony (C' white hashing) shows the EMT phases with corresponding section through the colony (C''m single yellow horizontal line). **(D)** 3D rendering of E14-Tg2A mESCs in Act/Chi, stained for fibronectin (green), phalloidin (red) and E-cadherin (white). Cells emerging from the colony secrete high levels of fibronectin and have altered F-actin architecture. E-cadherin is obscured due to the rendering process used to generate the 3D image. Individual channels are shown in (ii) illustrating membrane location of E-cadherin within the central colony; EMT initiation results in E-cadherin loss from the membrane. Fibronectin is observed on the basal surface of the colony. Scale bars represent 50 μm in **(A)** and 100 μm in **(B,C,D)**. Hoechst marks the nuclei in all images. AC, activin A + chiron; Act, activin A; Bra, brachyury; Chi, chiron CHIR99021; E-cad, E-cadherin; EMT, epithelial-to-mesenchymal transition; mESC, mouse embryonic stem cell; WT, wild type.

Bra expression. This sequence of events is reminiscent of an EMT, which characterize cells during the process of gastrulation. To investigate this further we probed for phenotypic landmarks of the EMT process in the differentiating cells (Figure 2B,C,D).

Pluripotent cells are characterized by high levels of E-cadherin [40-42] even though they lack an epithelial structure and when grown on gelatin, exhibit low levels of fibronectin basally (Additional file 2: Figure S2A,B). Analysis of fixed samples of cultures exposed to Act/Chi, shows that the onset of differentiation into mesendoderm is associated with a decrease in the levels of E-cadherin concomitant with the onset of Bra expression (Additional file 2: Figure S2A). The expression of Bra tends to be localized to the edges of the disorganizing colonies and coincides with a rearrangement of the actin cytoskeleton and a boundary of expression of fibronectin (see Figure 2C and Additional file 2: Figure S2C). As cells become motile, there is an increase in the amount of fibronectin basally, as well as a progressive increase in the levels of F-actin apically (Figure 2B,C,D and Additional file 2: Figure S2C). A proportion of F-actin is found in the lamellipodia and filopodia at the edges of the colony in what appears to be moving cells (Figure 2D and Additional file 2: Figure S2B).

These rearrangements of cellular elements are typical of an EMT and are very similar to those of cells moving into the primitive streak in embryos during stage E.7.5 (see Figures 2C and 3D in [43]) [44] suggesting that, under the influence of Act and Wnt signalling in culture, mESCs have activated a developmental programme very similar to that of cells undergoing gastrulation.

Brachyury expression correlates with Nanog expression during embryonic stem cell differentiation

A hallmark of ESC differentiation is the down-regulation in the expression of elements of the pluripotency network. To understand the relationship between this process and the onset of mesendodermal differentiation at the level of single cells, we used quantitative image analysis (QIA) to monitor the expression of Bra in wild-type (WT) E14-Tg2A mESCs relative to that of Nanog, Oct4 and Sox2 following Act, Chi or Act/Chi treatment (Figure 3 and Additional file 3: Figure S3).

Act treatment leads to the expression of Bra in a small proportion of the cells undergoing an EMT whereas either Chi- or Act/Chi-induced differentiation resulted in a larger proportion of cells expressing Bra and, eventually, adopting a mesenchymal morphology. Furthermore, in Act/Chi conditions, these cells also express Sox17 and FoxA2 and other primitive streak markers such as Gsc (data not shown). A small proportion of cells form tight balls around which the mesenchymal cells progressed (Figure 3A,B). The cells in the tight balls expressed Nanog, Oct4 and Sox2, suggesting that within the colony centres, the cells remain pluripotent. Confocal images from these samples were then subject to QIA where the average pixel intensity in cell nuclei (identified and segmented by Hoechst stain uptake levels) was measured for each fluorescent channel (Figure 3C-F).

Analysis of the time evolution of the distributions for the different proteins shows a wave of Bra expression in all conditions (Figure 3C), though it is more pronounced and involves more cells for Act/Chi. Chi alone also promotes the expression of Bra, but the levels and proportion of cells increase when it is supplemented with Act (Figure 3C). In both cases, the increase in Bra levels is far from homogeneous within the population of cells, a fact that is compatible with imperfect coordination of its rapid and transient expression. We also noticed that while the levels of Oct4 and Sox2 decrease during the first 2 days of differentiation (Figure 3E,F), in all cases Nanog expression undergoes a transient rise during days 2 and 3 (Figure 3D). Analysis of pairwise protein levels in individual cells indicates an increase in the correlation between Nanog and Bra levels in Act and Act/Chi conditions, which by day 2 go beyond the correlation levels in LB (Figure 3G). A more transient and earlier increase in correlation levels can be observed between Oct4 and Bra in Act/Chi. In addition, strong correlations were also observed between Nanog and Oct4 (Additional file 3: Figure S3), whereas Nanog and Sox2 became more correlated as time progressed (Additional file 3: Figure S3). These observations extend those of [45] and suggest that the events in culture parallel the events in embryos where there is a transient rise in Nanog expression in the cells of the primitive streak at the start of gastrulation [46-49].

These results, together with those of the cell behaviours associated with the differentiation process, suggest that exposure of mESCs to Act/Chi triggers a developmental process that is very similar to that of the cells that undergo gastrulation in terms of gene expression [34] as well as cell behaviour.

The onset of brachyury expression is tightly linked to an epithelial-to-mesenchymal transition and cell motility in adherent culture

Time-lapse imaging of Bra::GFP cells in different culture conditions (Figure 4A and Additional file 4: Figure S4A) and subsequent manual tracking of single cells (Figure 4B and Additional file 4: Figure S4B) allows us to simultaneously analyse the dynamics of Bra::GFP expression and the associated cell movement during the EMT, as well as the roles that Act and Wnt/β-catenin signalling have individually in these processes at the level of single cells (Figure 4 and Additional file 4: Figure S4; Additional file 5: Movie M1 and Additional file 6: Movie M2).

After 24 to 48 h of Act/Chi treatment, a large proportion of cells undergo EMT-like movements and become

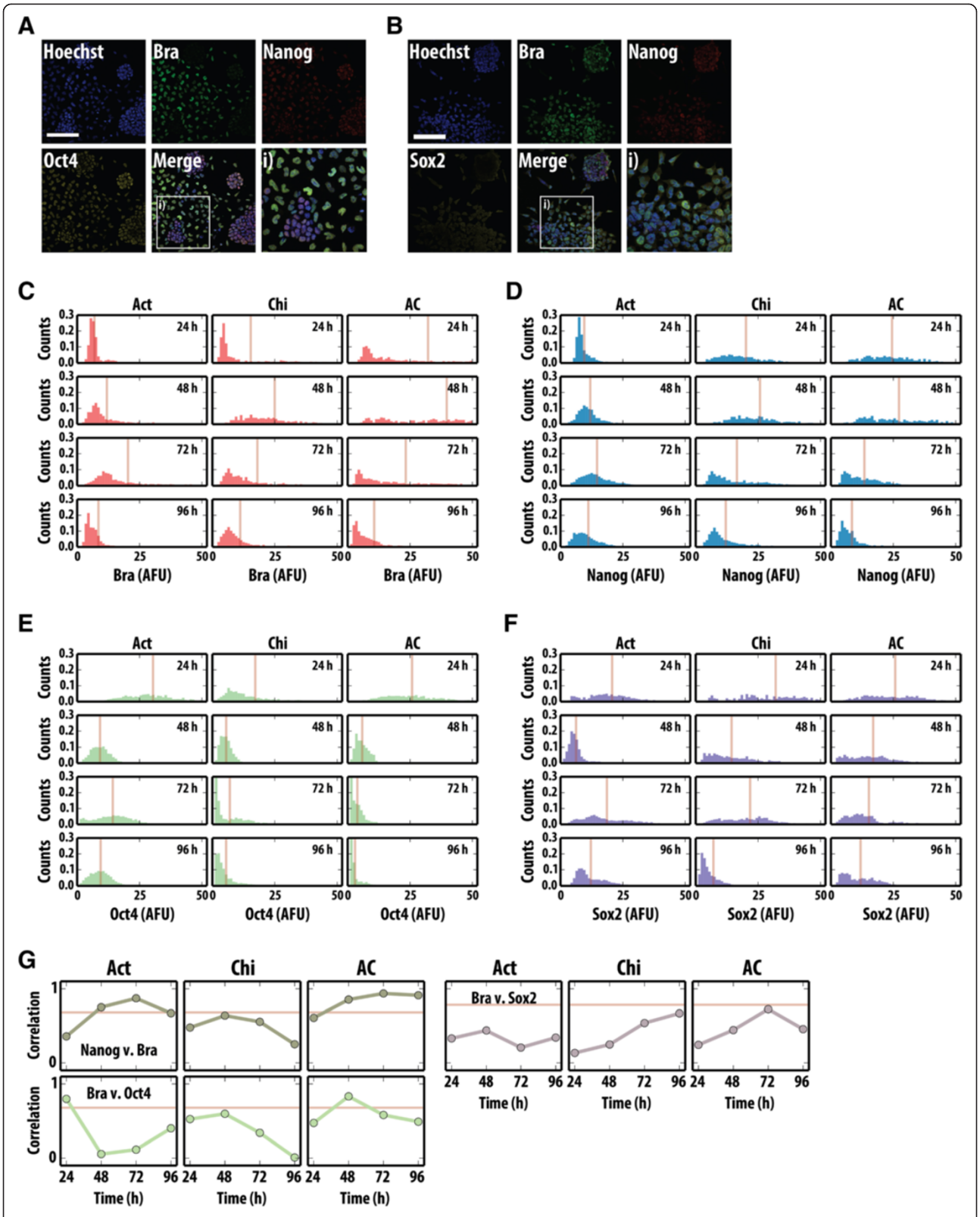

Figure 3 (See legend on next page.)

(See figure on previous page.)
Figure 3 Quantitative image analysis of Bra, Nanog and Oct4 or Sox2 following treatment with mesendodermal-inducing factors. **(A,B)** Confocal images of WT mESCs following 48 h Act/Chi treatment stained for brachyury (Bra; green) and Nanog (red) with either Oct4 **(A)** or Sox2 (**B**, yellow). Merged images are shown with the corresponding magnified regions denoted by a white box (i). **(C-F)** Time evolution of the distributions of the expression of brachyury **(C)**, Nanog **(D)**, Oct4 **(E)** and Sox2 **(F)** during differentiation. WT E14-Tg2A mESCs treated with Act, Chi or Act/Chi for 24, 48, 72 and 96 h were stained as described **(A,B)**. The nuclei were segmented based on Hoechst staining and the average pixel intensity for each fluorescent channel was quantified. The intensities for brachyury **(C)**, Nanog **(D)**, Oct4 **(E)** and Sox2 **(F)** are displayed as histograms for each time point. The bisecting orange lines in each histogram correspond to the mean fluorescence levels. **(G)** Pearson correlation coefficient for the correlations between Bra and Nanog (top left), Bra and Oct4 (bottom left) and Bra and Sox2 (top right) for the different time points. The horizontal line represents the correlation for LB. Scale bar represents 100 μm. Hoechst stain is used for the nuclei. AC, activin A + chiron; Act, activin A; AFU, arbitrary fluorescence units; Bra, brachyury; Chi, chiron CHIR99021; LB, leukaemia inhibitory factor and bone morphogenetic factor; mESC, mouse embryonic stem cell; WT, wild type.

openly motile (Figure 4A; Additional file 5: Movie M1). In these conditions, up-regulation of the Bra::GFP reporter was heterogeneous and occurred in cells that were in the process of or undergoing an EMT event within a temporally restricted window (Figure 4A). The time to the acquisition of a GFP-positive state was fixed, always spanning the second to early third day of differentiation. This correlation between Bra expression, EMT and movement is repeated when cells are treated with Chi or Act individually (Additional file 4: Figure S4A). In Act conditions, however, fewer cells up-regulated the Bra::GFP reporter (see Figure 1A) and the EMT-like events occurred between 48 and 72 h after initiation of treatment (Additional file 4: Figure S4A). Up-regulation of the reporter was on average more rapid in Act/Chi conditions than with either Chi or Act alone.

To quantify the characteristics of cell movement and GFP expression, individual cells were manually tracked for long periods of time at a high temporal resolution (approximately 6 frames/h, Figure 4B) and their Bra::GFP levels, instant velocities (the velocity of a cell from frame to frame) and motility (or diffusivity) were measured (Figure 4B'–G and Additional file 4: Figure S4B, C). Population-wise, cells in Act/Chi achieved higher instant velocities much earlier and sustained them for a longer period of time than in either Act or Chi alone (Figure 4B',D). Binning the velocities based on the time at which the cell analysis began (0 to 20 h, 20 to 40 h and 40 to 60 h), revealed that cells did not have high velocities from the very beginning but these built up as time progressed (Figure 4B',E).

Although the ability of Act or Chi to alter the instant velocities of individual cells was clear in our analysis, we resorted to statistical methods of random motion particle tracking to provide an objective measurement of the differences in cell motility between the different stimulation conditions (Figure 4D–G). In particular, we computed the mean-squared displacement (MSD) curves for each cell (Figure 4F), which, despite being less intuitive than cell velocities, provide a robust analytical framework for rapidly moving cells. When considering all cells tracked over the entire course of the experiment, the evolution of the MSD in Act/Chi is much higher than for individual Act or Chi stimulation (Figure 4E); i.e., cells treated with Act/Chi travel, on average, much larger distances in the same amount of time than cells in either Act or Chi. In addition, in the three cases (Act, Chi or Act/Chi), the initial MSD increases approximately linearly with time, a sign of diffusive movement, and after the first 3 h these plateau (Figure 4F). This levelling out of the MSD is due to a combination of both cell confinement as well as to the fact that we have only tracked cells that remain within the field of view (and thus we underestimate the MSD over long periods of time). Therefore, for each condition, we estimated an effective diffusivity (Additional file 4: Figure S4). The evolution of the coefficient of diffusion over time indicates that cells in Act/Chi acquire a much larger degree of motility than cells in Act or Chi and that they do so both much earlier and for a longer period of time (Figure 4G).

In addition, we studied the relationship between Bra expression and the dynamic behaviour of individual cells treated with Act/Chi. We found a correlation between Bra expression and cell movement and also that those cells with higher velocities had higher levels of the Bra::GFP (Figure 4C). Consistently, individual cells with levels of Bra::GFP above the average covered much larger ground (Figure 4C, lower panel).

We further analysed the trajectories of the cells to understand whether there was a particular bias to cell motion in terms of directionality and persistence (a continued direction of movement on a cell by cell basis; Figure 4H and Additional file 4: Figure S4D). In all conditions tested (including both an N2B27 and serum LIF control), the distribution of turning angles was far from isotropic (Additional file 4: Figure S4D; all conditions had $P < 0.00001$ for the Kolmogorov–Smirnov test against the uniform distribution), a clear indication that regardless of the medium condition, when cells move, they do so with persistence and that the main difference between different conditions is the velocity and the ground covered by individual cells (Additional file 4: Figure S4D).

The importance of Wnt/β-catenin signalling in the onset of Bra expression [50,51] (and here) led us to

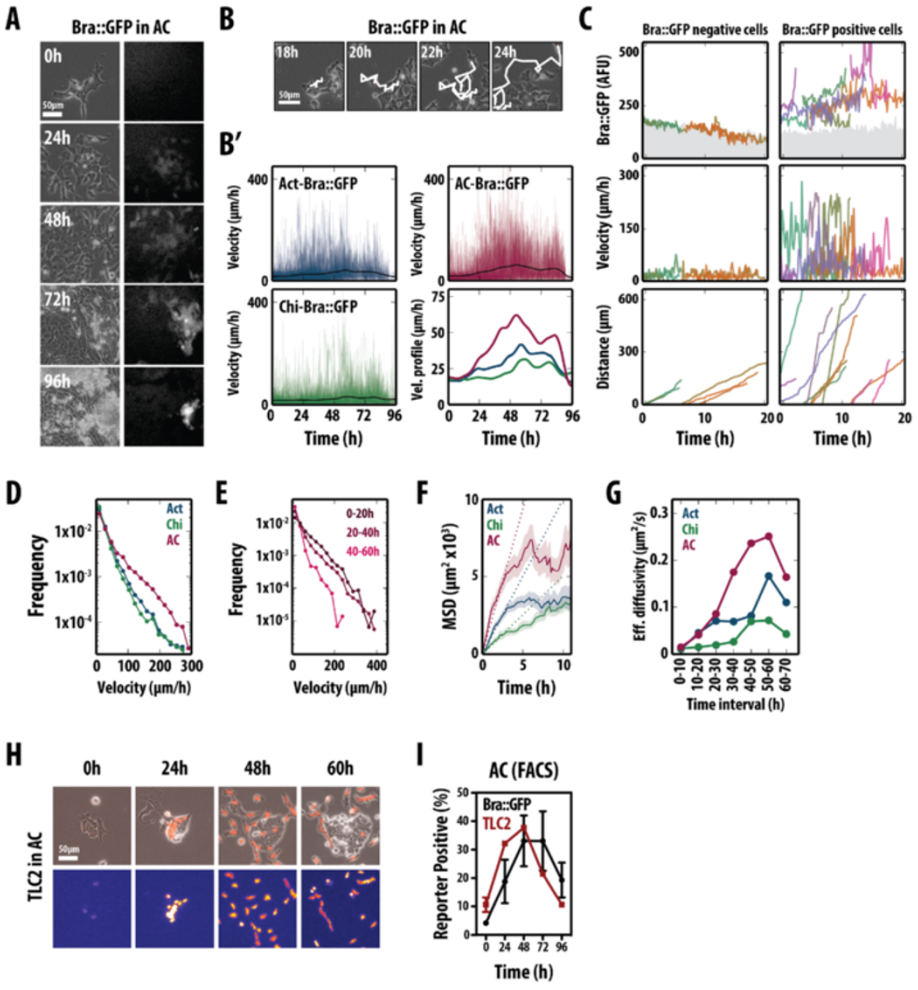

Figure 4 Live microscopy of Bra::GFP and a β-catenin transcriptional reporter (TLC2) following mesendodermal differentiation. (A) Stills from live imaging of Bra::GFP mESCs in Act/Chi (Additional file 5: Movie M1); phase contrast (left) and fluorescence (right). **(B,C)** Cells were manually tracked **(B)** and their velocities (**B'**, **C** middle), GFP expression (**C**, top) and distance travelled (**C**, bottom) were measured. Average velocities for all tracked cells in Act (blue), Chi (green) and Act/Chi (red) (**B'**, bottom right) show that cells in Act/Chi have on average the highest peak velocities, which are reached earlier. **(C)** Each cell represented by a colour showing that all cells move, but only cells that express Bra move with a high velocity. There seems to be a relationship between the levels of Bra expression, velocity and distance travelled by individual cells. **(D)** Distribution of individual cell velocities under different conditions. Cells in Act/Chi have a higher proportion of fast movers. **(E)** Cell velocity increases with time. **(F)** Mean-squared displacement (MSD) curves representing the range of individual movements of all cells tracked over the whole experiment. **(G)** Effective diffusion coefficients at different time intervals. Coefficients were estimated by fitting straight lines to the MSD curves obtained when considering cells at different 10 h intervals. **(H)** Live imaging of the TLC2 Wnt/β-catenin reporter in Act/Chi (Additional file 6: Movie M2). Differentiation results in reporter up-regulation before cells initiate the EMT and down-regulation as cells leave the colonies. **(I)** FACS analysis of Bra::GFP and TLC2 reporters revealing activation of β-catenin transcriptional activity relative to activation of Bra within a population of cells. Average of three replicate experiments ± standard deviation. Scale bars represent 50 μm. AC, activin A + chiron; Act, activin A; Bra, brachyury; Chi, CHIR99021; FACS, fluorescence-activated cell sorting; Eff., effective; GFP, green fluorescent protein; MSD, mean-squared displacement.

monitor Wnt/β-catenin signalling during differentiation using an H2B-TCF/LEF-mCherry reporter over time (TLC2) (Figure 4H,I and Additional file 4: Figure S4E) [52,53]. Cells initially expressed low, heterogeneous levels of fluorescence. Over time, however, reporter expression increased within the centre of colonies until cells began to disperse from the edges as they initiated EMT (Figure 4H, Additional file 4: Figure S4E and Additional file 6: Movie M2). The activity of the Wnt-reporter in the transitioning cells was down-regulated following their exit from the colony, correlating with Bra::GFP down regulation in highly motile cells (Figure 4I and Additional file 4: Figure S4E).

Our observations and analysis provide information on the temporal order of events with respect to Bra

induction, β-catenin signalling and the EMT: (a) cells increase the β-catenin transcriptional activity, (b) cells express Bra and initiate the EMT event and (c) cells reduce transcriptional activity of β-catenin and Bra as cells migrate away from the colony and become motile.

Nodal/activin and Wnt/β-catenin signalling provide a link between the epithelial-to-mesenchymal transition and Bra expression

Our observations reveal a close relationship between the onset of Bra expression, the associated EMT and the activation of Wnt signalling. To establish a functional relationship between these three events, we first used cyclosporine A (CsA) to inhibit the EMT during the differentiation process and assessed the expression of Bra::GFP by FACS (Figure 5A). CsA has been shown to inhibit calcineurin thereby preventing both the phosphorylation and therefore the activation of nuclear factor of activated T-cells (NFAT) [54,55] and the transition from an epithelial towards a mesenchymal state [56]. In our experiments, CsA delayed the onset of Bra::GFP expression induced by Act alone and reduced the number of GFP-positive cells to a maximum of <10% at the end of the treatment (Figure 5A). For Chi, CsA resulted in an immediate reduction of Bra::GFP expression throughout the whole period of observation to levels similar to those observed with Act and CsA (Figure 5A). Although simultaneous Act/Chi and CsA treatment showed an initial decrease in the proportion of GFP-positive cells after 24 h, CsA treatment appeared only to delay the onset of Bra::GFP induction and shift the GFP-positive distribution by 48 h (Figure 5A).

In the presence of Chi, E14-Tg2A cells exhibit a loss of E-cadherin from the membrane and nuclear relocalization of β-catenin coincident with the EMT and the onset of Bra expression (Figure 5B,B' and Additional file 2: Figure S2A). Instead, cells in both Chi and CsA did not lose E-cadherin expression and for the most part, β-catenin remained associated with the membrane (Figure 5B,B''). Cells in these conditions display low expression of Bra and of Bra::GFP (Figure 5A,B,B'') and show that a release of β-catenin from the adherens junctions is a prerequisite for its effect on Bra expression. On the other hand, cells treated with Act and CsA showed limited upregulation of Bra (the same as we observe with Bra::GFP), with incomplete degradation of E-cadherin (Additional file 7: Figure S5A). However, CsA had a much lesser effect in the presence of Act/Chi resulting in similar, though delayed, E-cadherin and membrane β-catenin degradation compared to the DMSO control, and expression of Bra (Figure 5A and Additional file 7: Figure S5B). The combined effect of Act/Chi on Bra expression although unintuitive can be interpreted as following: Act loosens the adherens junctions, which releases a small amount of β-catenin from the membrane, and Chi amplifies this effect. However, when CsA is added in the presence of Chi, very little β-catenin can be released from the membrane since higher concentrations of Act are required for this process. In Act and CsA without the addition of Chi, there is no feedback (i.e. from Wnt secretion mediated by β-catenin), since β-catenin remains in the membrane. Finally, CsA in the presence of Act/Chi simply delays the EMT since the concentrations of Act/Chi are eventually sufficient to bypass the inhibitory effect of CsA.

Live imaging of cells under these conditions revealed that although cells treated with either Act or Chi in the presence of CsA begin to form membrane protrusions such as lamellipodial and filopodial projections, suggestive of EMT initiation ([57] and as confirmed with immunofluorescence), they remained within tight colonies and did not become motile (Figure 5B,C). This is supported by the quantitative analysis of the cell movements over time (velocities; Figure 5D,E and Additional file 7: Figure S5C), which revealed that cells treated with CsA are unable to show the rapid cell motion observed in the DMSO controls, even in the presence of Act/Chi, and were more likely to move under 36 μm/h (the basal velocity of cells) for prolonged periods of time and were retarded in their ability to engage in large cell-steps under all conditions (Figure 5D,E).

These results, taken together with the inhibitor studies using SB43 (Figure 1A), suggest that activation of Bra transcription is dependent on: (a) the ability of individual cells to execute an EMT program, (b) the loss of E-cadherin at the cell surface and (c) the concomitant nuclear translocation of β-catenin. Consistent with this conclusion, β-catenin$^{-/-}$ mutant cells and cells harbouring a transcriptionally inactive β-catenin, β-catenin$^{\Delta C/-}$, were unable to express Bra in the presence of Act and Chi (Figure 6A,B). Time-lapse imaging revealed striking differences between the two β-catenin mutant cell lines and WT (Figure 6C). Whereas by 24 h both the E14-Tg2A and β-catenin$^{-/-}$ mESCs began to show signs of the initiation of the EMT (dispersing cells with a mesenchymal appearance), the β-catenin$^{\Delta C}$ cells remained tightly associated within their colonies (Figure 6C). As time progressed, the β-catenin$^{-/-}$ cells showed a much greater reduction in viability compared to the E14-Tg2A control and became motile (albeit much slower); however, they remained within close proximity to the colony from which they were dispersing (Figure 6B). Manual tracking of these cells revealed that the speed at which cells move, and thereby indirectly the distance covered, over the time course was significantly shorter than the E14-Tg2A control, with a velocity much less than 36 μm/h for most of the time course (Figure 6D, E, Additional file 8: Figure S6A). Unlike the E14-Tg2A control, the β-catenin$^{\Delta C}$ cell colonies at the initiation of

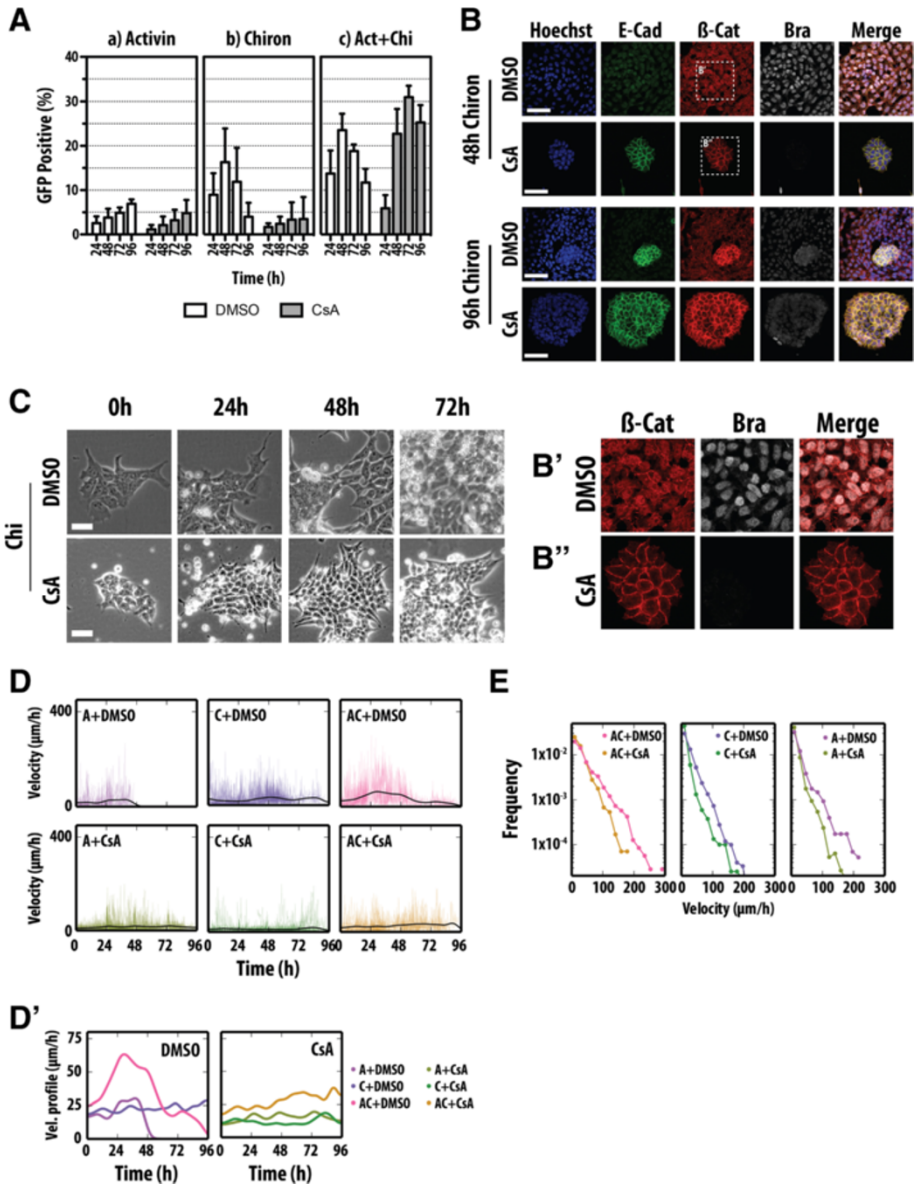

Figure 5 An EMT event is required for Bra::GFP expression. (A) Expression of Bra::GFP in mESCs subject to (a) Act, (b) Chi and (c) Act/Chi, in the presence of CsA (3 μM; grey) or vehicle (DMSO; white) analysed by FACS. Error bars show standard deviation, $n = 3$. **(B,B',B")** E14-Tg2A mESCs subject to Chi in the presence of CsA (3 μM) or DMSO, stained for Hoechst, E-cadherin, β-catenin and Bra. Scale bars denote 50 μm. In the presence of CsA, E-cadherin is not effectively cleared from the membrane, β-catenin does not enter the nucleus and there is no effective expression of Bra. **(C)** Stills from live imaging of E14-Tg2A mESCs in Chi with DMSO or CsA. Notice that in CsA, cells stretch out filopodia but do not undergo an EMT. Scale bars denote 50 μm. **(D)** Cell velocities (μm/h) measured from multiple films as in **(C)**. Tracking for Act + DMSO ceased after 48 h due to loss of focus. Refer to Figure 4 for comparison. Analysis of the average instant velocities shows that CsA reduces the movement of the cells. **(E)** Distribution of instant velocities. AC, activin A + chiron; Act, activin A; β-cat, β-catenin; Bra, brachyury; Chi, chiron CHIR99021; CsA, cyclosporine A; DMSO, dimethyl sulfoxide; E-Cad, E-cadherin; EMT, epithelial-to-mesenchymal transition; GFP, green fluorescent protein; Vel. velocity.

imaging (90% of the colonies of cells present at the initiation of imaging) formed tight, spherical colonies not dissimilar to those observed in 2iLIF conditions (Figure 6C). Due to the high degree of compaction within the cell balls of the β-catenin$^{\Delta C}$ mutant line, single cells could not be followed for periods of time to allow comparison of their velocities with the other mutant lines and the E14-Tg2A controls. The appearance of the colonies is probably due to enhanced E-cadherin-mediated adhesion in these cells.

These results, in combination with the chemical genetics approach above, revealed that partial or complete loss of β-catenin and disruption of its transcriptional activity impair the ability of ESCs to both up-regulate and

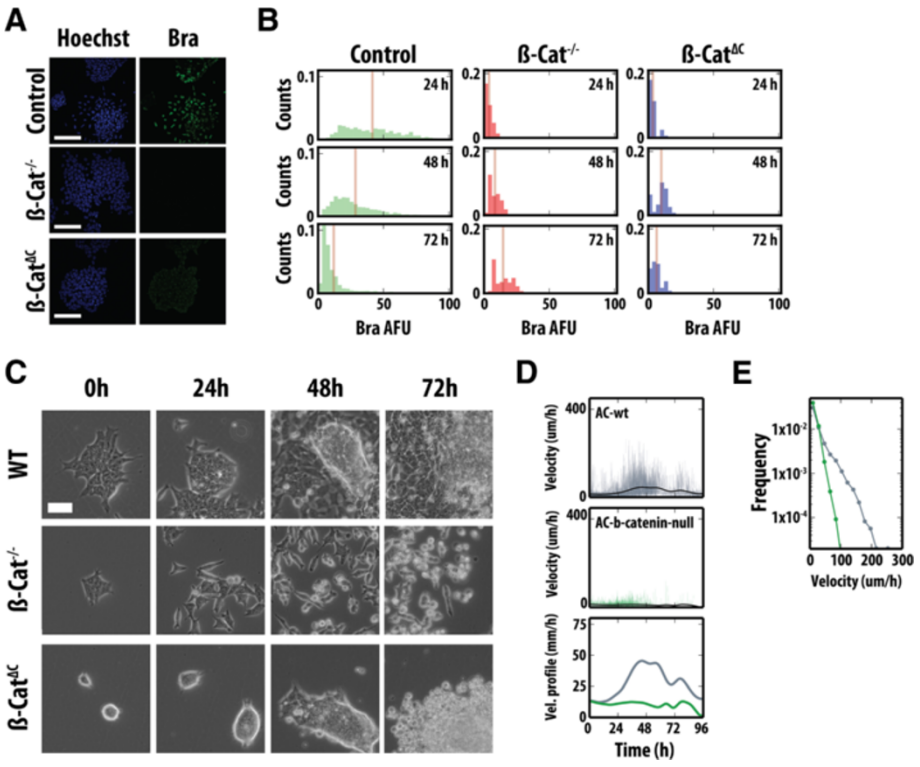

Figure 6 β-catenin transcriptional activity and expression of Nanog are required for Bra expression and associated EMT. (A) Bra expression in E14-Tg2A, β-catenin$^{-/-}$ and β-catenin$^{\Delta C}$ cells differentiated in Act and Chi. Hoechst stain is on the left-hand side. **(B)** Time evolution of the distribution of Bra expression in cells as in **(A)**. β-catenin transcriptional activity is required for Bra expression. See text for details. **(C)** Live imaging of β-catenin mutants in Act/Chi. **(D)** Individual cell velocities (μm/h), and the average velocity profile for each cell line (indicated by colours) in Act/Chi. **(E)** The distribution of velocities over time. Scale bars denote 50 μm. Act, activin A; AFU, arbitrary fluorescence units; β-cat, β-catenin; Bra, brachyury; Chi, chiron CHIR99021; EMT, epithelial-to-mesenchymal transition; Vel., velocity; WT, wild type.

undergo specification towards a primitive-streak-like fate.

Nanog is required for the effect of brachyury on the epithelial-to-mesenchymal transition

Our previous analysis on the correlations between Nanog and Bra expression (Figure 3D,G) and a previous investigation of human ESCs detailing Nanog regulation of Bra [58] led us to follow the ability of Nanog$^{-/-}$ mESCs to express Bra and undergo EMT by both live-cell imaging and QIA (Additional file 8: Figure S6). QIA analysis shows that following differentiation in Act/Chi, Nanog$^{-/-}$ mESCs express much lower levels of Bra and Sox2 (Additional file 8: Figure S6B). Live imaging of these cells by widefield microscopy revealed that they undergo an EMT (Additional file 8: Figure S6C), although subtle differences can be observed in the dynamics of cell movements and in the morphology associated with their differentiation (Additional file 8: Figure S6C,D,E): analysis of the instant velocities revealed that Nanog$^{-/-}$ mESCs were less likely to engage in rapid velocities compared with the WT cells although not to the same extent as the β-catenin$^{-/-}$ line (Additional file 8: Figure S6D,E). These observations suggest that Nanog facilitates the up-regulation of Bra, though its presence is not a requirement for the initiation of the EMT program.

Brachyury expression is required for rapid cell movement following an epithelial-to-mesenchymal transition

In the embryo, the absence of Bra leads to truncation of the body axis and defects in axial extension, but does not have a major phenotype during gastrulation until the formation of the node (E7.5) [10,22]. This led us to test the behaviour of Bra mutant cells in the context of ESC differentiation; in particular, we asked whether the EMT program is activated as a consequence or is independent of the initiation of Bra transcription. To test this we analysed the properties of Bra$^{-/-}$ mESCs in culture (Figure 7).

In all conditions, Bra$^{-/-}$ cells were able to display the characteristics of an EMT, although the proportion of cells undergoing these changes appeared lower than the WT cells and the process was defective. In the presence of Act and Chi, although mutant lines were able to display movements associated with an EMT, immunofluorescent

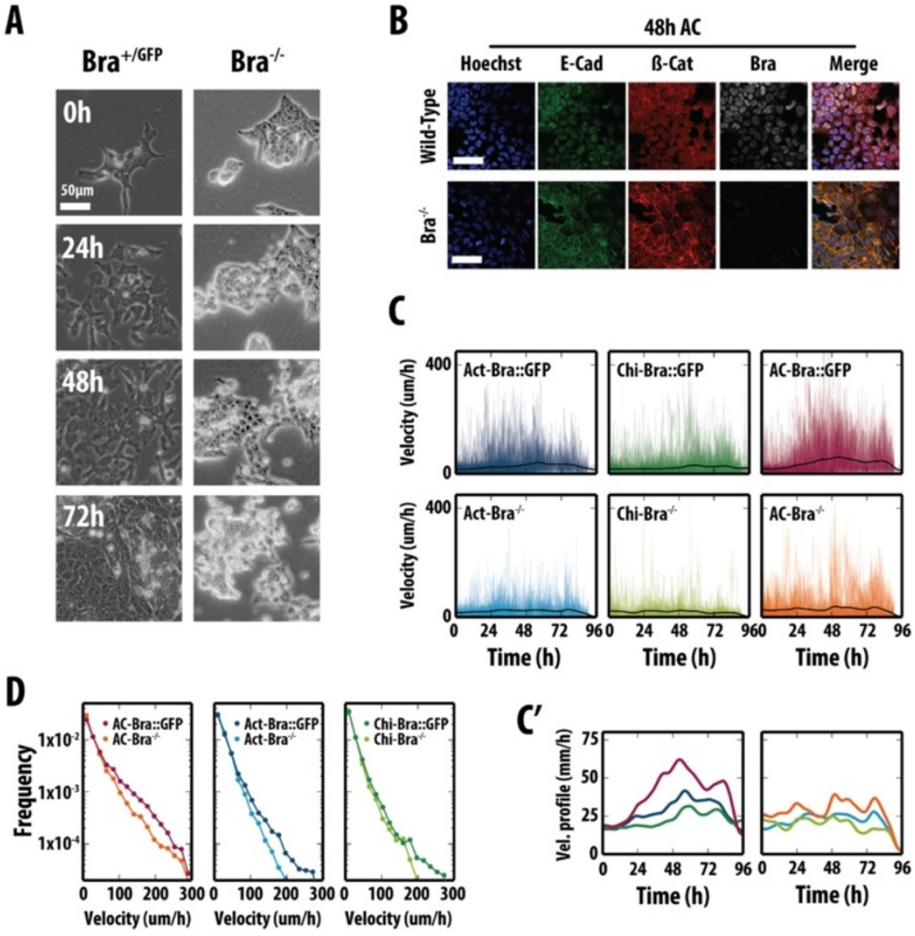

Figure 7 Bra is required for an EMT event during mesendodermal differentiation. (A) Phase-contrast images from live imaging of Bra::GFP ($Bra^{+/GFP}$) and $Bra^{-/-}$ mESCs in Act and Chi. Bra::GFP stills were shown in Figure 4A. In the absence of Bra, cells do not undergo a full EMT. **(B)** E14-Tg2A and $Bra^{-/-}$ mESCs after 48 h in Act and Chi, immunostained for E-cadherin, β-catenin and Bra and imaged by confocal microscopy. Scale bars indicate 50 μm. Hoechst stain marks the nucli. In the absence of Bra, E-cadherin and β-catenin are not effectively cleared from the membrane. **(C,C')** Instant velocities of Bra::GFP cells and Bra null cells in Act, Chi or Act/Chi. The thick black line in the individual graphs indicates the average velocity for each condition, and is displayed in greater detail in **(C')**. **(D)** Histograms of instant cell velocities as measured from frame-to-frame displacements for both Bra::GFP and $Bra^{-/-}$ mESCs. All the Bra::GFP live imaging data was displayed in Figure 4. AC, activin A + chiron; Act, activin A; Bra, brachyury; Chi, chiron CHIR99021; Eff., effective; EMT, epithelial-to-mesenchymal transition; FACS, fluorescence-activated cell sorting; GFP, green fluorescent protein; mESC, mouse embryonic stem cell.

staining revealed that in most cells, the degradation of E-cadherin and the subsequent nuclear localization of β-catenin were impaired (Figure 7B). Nonetheless, by 48 h there was a clear decrease of E-cadherin in the membrane and some β-catenin above background in the nuclei (Figure 7B). Manual tracking of the mutant cells over the time course revealed their average instant velocity in Act and Act/Chi to be slower than the control Bra::GFP cells (Figure 7C,D and Additional file 9: Figure S7; Bra::GFP cells from Figure 4) and therefore the distance travelled per time step was less than for the control cells (Figure 7D). Interestingly, the effect of Chi on the Bra mutant cells was not as pronounced as that seen in Act or Act/Chi conditions: the probability of generating high velocities with Bra mutants was similar to the control cells with Chi treatment (Figure 7D).

These observations indicate that Bra is not necessary for the EMT, but functions to promote high-velocity motion within Bra-expressing cells, possibly facilitating their exit from the primitive streak. Together with the inhibitor studies and live-cell imaging of reporter cell lines, these data suggest that Bra, under the control of β-catenin, modulates the instant velocities of the cells as they enter the primitive streak fate and may control the expression of a factor or factors that allow progression of the EMT and therefore specification of the primitive streak. It also shows that, for the most part, the effect of Chi on cell movement is not significant and is independent of Bra expression.

Discussion

It is thought that ESCs provide a unique model system for interrogating developmental processes in culture [59,60]. However, this possibility rests on the assumption that processes in tissue culture mimic events in the embryo and this has not yet been adequately tested. Here we have applied a combination of live-cell microscopy, QIA and FACS to investigate the onset and consequences of Bra expression in differentiating mESCs and analyse to what extent they reflect related events in embryos. In contrast to earlier studies, which have been performed at the level of bulk populations of differentiating cells and mostly focused on gene expression, we have analysed the dynamics and correlation between gene expression and cell behaviour at the level of single cells. Our idea is to compare the events in culture with the specification and morphogenetic activity of a related population of cells in the embryo: the primitive streak.

In the mouse embryo, the expression of Bra is tightly linked to the process of gastrulation and body extension, in particular, to a population of cells in the epiblast that experience a wave of EMTs associated with directional movement [13-15]. This population sows the precursors for the definitive endoderm and the mesoderm and plays a central role in laying down the axial structure of mammalian embryos [6,12,19,61]. Throughout gastrulation, Bra is expressed transiently within a moving population of cells, and a similar pulse of expression has been inferred from FACS analysis of cultured ESCs under the influence of Act and β-catenin signalling [8,29,34]. We have confirmed this observation and extended it by showing that the onset of Bra expression is autonomous in cells and that, like in the embryo, it is associated with an EMT [4,6,15]. Furthermore, we observe in culture that after the EMT, as cells become migratory, they lay down an extracellular matrix (ECM) over which they move. This situation mimics the embryo where cells move over a bed of fibronectin, which has been shown to be important for fate specification [39,62,63]. In the embryo, it is difficult to resolve the source of the fibronectin, as it could be the epiblast or the ingressing cells. Our results would suggest that it is the ingressing cells that have expressed Bra that make an important contribution to laying down the ECM.

In mESCs the expression of Bra is confined to a narrow temporal window, between days 3 and 4. If one assumes that mESCs are in a state similar to that of the pre-implantation blastocyst (stage E4.0), the timing of Bra expression in differentiating mESCs, 2 days later, is similar to that of embryos between E6.5 and E7.0, the time at which gastrulation commences [6,64]. There are other features of the process in culture that parallel events in the embryo. In particular, the association of Bra expression with β-catenin signalling [50,53,65], an EMT and the coexpression of both Nanog and Oct4 with Bra during these processes [45,66]. There are reports that in human ESCs, Nanog is required for Bra expression [58] and here we have shown that the same is true in mESCs where the absence of Nanog dramatically reduces the expression of Bra and affects the behaviour of the cells.

Altogether, our observations support and extend the notion that *in vitro* differentiation of ESCs into a Bra-expressing population, exhibits several parallels with the definition and behaviour of the primitive streak during mammalian gastrulation beyond gene expression profiles [34,67]. This opens up the possibility of using ESCs to probe the molecular mechanisms linking cell fate and cell behaviour and, by comparing the evolution of the processes in cells and embryos, gain some insights into the emergence of collective behaviour from the activities of single cells.

Our results suggest an interplay between Act and Wnt/β-catenin signalling, the EMT and the activity of Bra in the specification and behaviour of cells in the primitive streak. Act initiates the EMT and the expression of Bra. The EMT triggers Wnt/β-catenin signalling, which enhances the effect of Act on Bra, which, in turn, promotes cell movement and cell fate [68,69]. This module has the structure of a feed-forward loop. In agreement, Bra has been shown to control the expression of several components of the cytoskeleton and canonical/non-canonical Wnt signalling [65,70-72], which are likely to promote movement and enhance the EMT. Downstream targets of Bra comprise members of the Wnt family, which are likely to fuel movement. It is possible that the sluggish movement that we observe in the absence of Bra, is due to the activation of β-catenin by Chi, which might set in motion some of these mechanisms in a Bra-independent manner. In the absence of other elements, also controlled by Bra, the movement is greatly hampered.

A tissue culture model for primitive streak formation?

Differences between the events in the embryo and those in differentiating mESCs can be informative. An example is provided by the long-range movement that we observe in differentiating mESCs, which is not obvious in the embryo. During gastrulation, after their EMT, cells expressing Bra do not display long-range movement as individuals but rather jostle as a group towards the proximal posterior pole and then ingress through the primitive streak [15]. However, when they are explanted and placed onto ECM-covered culture dishes, the same cells can be observed to move individually, without a preferred direction but with some persistence/diffusivity [73] in a manner that is very reminiscent to what we have described here for differentiating mESCs. These observations suggest that the main difference between Bra-expressing mESCs and those

in the embryo, is the confinement of the latter, which restricts their movement and forces them to behave as a coherent collective, rather than becoming dispersed individual cells, as they do in the culture. It is interesting that the average velocity of the differentiating ESCs cells in Act/Chi (maximum average instant velocity of approximately 60 μm/h; Figure 4B') is within the same order of magnitude as that of the cells from primitive streak explants (average of 50 μm/h on ECM-coated surfaces) [73] and of migrating mesodermal cells within the embryo (46 μm/h) [74]. It is important to note that in our experiments, we were only able to see a small proportion of cells, which were able to travel at approximately 400 μm/h, albeit for short durations of time (Figure 4B').

We observe a correlation between the level of Bra and the velocity of the cell. Bra mutant cells are very much delayed in migrating. Only a few do migrate and when they do, they exhibit lower velocities relative to WT. Similar observations have been made for cells from Bra mutant primitive streaks [73] and indicate that an important function of Bra is to control the movement of the cells. On the other hand the combination of Act and chi promotes very high velocities, which, in the confinement of the embryo, can result in strong directional forces. It is important to note that other transcription factors may be required in addition to Bra for the sustained movement of cells out of the primitive streak. In support of this, mice deficient of *msgn1*, a direct target of Bra [75], have an enlarged tail bud and cells have defects in their ability to migrate away from the primitive streak [76].

These observations emphasize the importance of confinement in the behaviour of the cells in the primitive streak. At the onset of gastrulation, the epiblast is a highly packed dividing cell population. At this stage, movement towards and through the streak is likely to be due to large-scale, spatially constrained tectonic movements of the epiblast as a whole, with mechanical differences between the prospective anterior and posterior parts being responsible for the directional movement of the bulk population that has undergone EMT. Indeed imaging gastrulation in mouse embryos suggests that once cells have undergone EMT, Bra-expressing cells are pushed towards the streak in a process that appears to be passive and not require convergence and extension, as appears to be the case for frogs and fish [15]. This notion of morphogenetic events underpinned by long-range mechanical coordination of cells within tissues has been demonstrated during the convergence and extension movements of the neuroectoderm in the development of the nervous system in zebrafish [77]. Such long-range effects might provide an explanation for the lack of a clear phenotype of Bra mutant cells during gastrulation. While this is likely to be the result of partial redundancy with eomesodermin [78-80], it might be also be a reflection that at these early stages, the defects of Bra mutant cells are compensated by, mechanical large tissue coordination due to confinement. Bra mutant cells still undergo an EMT and therefore could be subject to these movements. As we have shown here, Bra mutant cells can initiate an EMT and therefore could be the subject of strong large-scale forces, which are likely to exist throughout the epiblast. After node formation, however, the strength of these forces might subside and regressing cells, particularly during axis extension, may come to rely more on the propulsion and navigational abilities driven by Bra. This is supported by the behaviour of mosaics of cells with different levels of Bra in WT embryos [10,23,61] and by our observation of a correlation between levels of Bra expression and cell velocity. Also, in agreement with this, WT cells are outcompeted by cells expressing higher levels of Bra in the early gastrula [61]. Therefore, cells with higher motility might be more prone to escape the tectonic movements of the tissue and can 'overtake' WT cells.

Conclusions

Our results highlight the experimental possibilities provided by differentiating ESC as a first approximation to understanding the mechanisms underlying events that, like gastrulation, are difficult to access in the embryo. Having established the similarities between the two systems, it will be important to exploit them to see how one could reproduce the primitive streak in culture through, for example, confining the movement of differentiating ESCs and attempting to create directionality by imposing spatially constrained forces.

Methods

Routine cell culture and primitive streak differentiation

E14-Tg2A, Bra::GFP [8], $Bra^{-/-}$ [10], TLC2 [53] and $Nanog^{-/-}$ [48] mESCs were cultured on gelatin in serum and LIF (ESLIF). β-$catenin^{-/-}$ and β-$catenin^{\Delta C}$ mESCs [81] were cultured in 2iLIF [32] on fibronectin. For differentiation assays, cells were plated in ESLIF (6×10^3 cells/cm^2) and 24 h later the medium was replaced with N2B27 [30] (NDiff 227, StemCells Inc., Cambridge, UK) supplemented with LB. Cells were differentiated 24 h later in N2B27 with combinations of Act (100 ng/ml), Chi (3 μM) or dual stimulation (Act/Chi). Differentiation of β-$catenin^{-/-}$ and β-$catenin^{\Delta C}$ lines omitted the LB stage. Small molecule inhibitors used were: 1 μM XAV939 [82], 1 μM IWP3 [83], CsA [55] (5 μM), 10 μM SB43 [84] and 0.2 μM dorsomorphin (DM) [85]. If cells were not being passaged, they were fed daily by replacing half the medium in the tissue culture flask with fresh growth medium. The cells used here are all 129 strain derived from C57BL/6

mice and we did not see any qualitative differences for when they exhibited the different morphogenetic behaviours or the way they moved or differentiated. We therefore expect a lower degree of variation between these and control lines than between other WT cells not derived from C57BL/6 mice.

Fluorescence-activated cell sorting analysis

GFP (Green Fluorescent Protein) and RFP (Red Fluorescent Protein) was assessed using a Fortessa flow cytometer (BD Biosciences, Oxford, UK). Analysis of data from single, live cells (4',6-diamidino-2-phenylindole (DAPI)-negative) was conducted using Flowjo software (Tree Star, Inc, Oregon, USA). The GFP-positive populations from FACS data were analysed using a one-way ANOVA with Tukey's adjustment comparing the time-matched DMSO control and treatment. Significance was set at $P < 0.05$.

Quantitative image analysis and confocal microscopy

Immunofluorescence and image analysis were carried out as described previously [86] in eight-well (Ibidi, Thistle Scientific LTD, Glasgow, UK), plastic tissue-culture dishes, within 200 μl medium/well. Primary antibodies are as follows: goat-anti-Bra (Santa Cruz Biotechnology Inc., Heidelberg, Germany, sc-17743), rabbit-anti-β-catenin (total β-catenin, Sigma-Aldrich Company LTD., Dorset, UK, C2206), rat-anti-E-cadherin (Takara Bio Europe/SAS, Saint-Germain-en-Laye, France, M108), rabbit-anti-fibronectin (Abcam, Cambridge, UK, 2413), rat-anti-Nanog (eBiosciences Ltd, Hatfield, UK, 14–5761), mouse-anti-Oct3/4 (Santa Cruz, N3038) and rabbit-anti-Sox2 (Millipore, Dundee, UK, AB5603). Alexa-conjugated phalloidin (Invitrogen, Paisley, UK) and Hoechst3342 (Invitrogen) were used to stain F-actin and nuclei, respectively. Alexa-conjugated secondary antibodies were from Invitrogen. Samples were imaged using an LSM700 on a Zeiss Axiovert 200 M with a 40× EC Plan-NeoFluar 1.3 NA DIC oil-immersion objective. Hoechst3342, Alexa-488, −568 and −633/647 were sequentially excited with 405, 488, 555 and 639 nm diode lasers respectively. Data capture was carried out using Zen2010 v6 (Carl Zeiss Microscopy Ltd, Cambridge UK) and image analysis performed using Fiji [87].

Widefield live-cell microscopy and analysis

For live imaging, cells were imaged by widefield microscopy in a humidified CO_2 incubator (37°C, 5% CO_2) every 10 minutes for up to 96 h using a 20× LD Plan-Neofluar 0.4 NA Ph2 objective with correction collar set to image through tissue-culture plastic dishes. Illumination was provided by an LED white-light system (Laser2000, Kettering, UK). The filter cubes GFP-1828A-ZHE (Semrock, NY, USA) and Filter Set 45 (Carl Zeiss Microscopy Ltd. Cambridge, UK) were used for GFP and RFP respectively. Emitted light was recorded using an AxioCam MRm and recorded with Axiovision (2010) release 4.8.2. Analyses were performed using Fiji [87] and associated plugins: MTrackJ [88] or Circadian Gene Expression (CGE) [89,90]. When MTrackJ was used, the bright-field channel from the live-cell imaging was used to identify cell nuclei manually, the centre of which was used as a seed point for the position of the cells. Single cells were then tracked until they divided, became obscured by other cells or left the field of view. Additional file 10: Table S1 summarizes the tracking data collected. To measure the level of reporter expression, a small circular region of interest of radius 10 μm was automatically generated around the centre of each cell and the average pixel intensity from the fluorescence channel was recorded. Movies not included in the supplementary data are available upon request.

Quantitative RT-PCR analysis

Cells were harvested at the relevant time points. RNA was extracted in TRIzol (Life Technologies, UK) and purified using the Qiagen RNeasy Mini Kit (Qiagen). Complementary DNA (cDNA) synthesis was performed with 1 μg of total RNA extract using the SuperScript III First-Strand Synthesis System (Life Technologies). RNA was digested afterwards with RNaseH. PCR reactions were run in triplicate using 12.5 μl QuantiFAST SYBR Green Master Mix (Qiagen), 3 μl cDNA, 0.5 μl primer mix (50 μM) and 9 μl dH_2O. Pipetting was performed automatically by QIAgility (Qiagen). Initial sample concentrations were estimated using an in-house adapted MAK2 method [91]. Technical repeats were averaged and normalized to GAPDH levels. Standard errors were propagated accordingly. Primer pairs are as follows: brachyury forward CTGGGAGCTCAGTTCTTTCG, reverse GTCCACGAGGCTATGAGGAG; GAPDH forward AAC TTTGGCATTGTGGAAGG, reverse GGATGCAGGGA TGATGTTCT. Cycling conditions: initial denaturation at 95°C for 5 minutes, followed by 45 cycles of denaturation at 95°C for 10 seconds and combined annealing and extension at 60°C for 30 seconds. Melt curves were generated between 60 and 95°C, holding for 5 seconds for each temperature step.

Additional files

Additional file 1: Figure S1. Cells cultured in N2B27 are unable to express the Bra-GFP reporter. Bra::GFP mESCs were plated and differentiated for 48 h in either N2B27 supplemented with Act/Chi (positive control; blue line left panel) or in N2B27 (red line, right panel) without any other factors. The percentage of GFP-positive cells for Act/Chi or N2B27 conditions are shown. An E14-Tg2A WT control is displayed in each panel (tinted grey profile). AC, activin A + chiron; Bra, brachyury; GFP, green fluorescent protein; WT, wild type.

Additional file 2: Figure S2. Status of brachyury, E-cadherin, fibronectin and F-actin in pluripotent and differentiating E14-Tg2A mESCs. **(A)** E14-Tg2A mESCs in LB or differentiated in Act and Chi for 48 h, stained for Bra (green)

and E-cadherin (E-Cad; red) and imaged by confocal microscopy. Act and Chi treatment alters Bra expression and causes a loss of E-cadherin from the membrane. **(B)** E14-Tg2A mESCs cultured in serum and LIF, stained for fibronectin (green) and with phalloidin to mark F-actin (red). The pluripotent state is characterized by low fibronectin and F-actin localized to cell–cell boundaries, lamellipodia and protruding filopodia; see magnified region (i). **(C)** A montage illustrating the z-section (in 1 μm increments) of the colony imaged in Figure 2C and Figure S2D showing all fluorescent channels merged (top left), Hoechst stain and fibronectin (top right), Hoechst stain and Bra (bottom left) and Hoechst stain and phalloidin (bottom right). Hoechst stain, fibronectin, brachyury and phalloidin are coloured blue, green, white and red respectively. See main text for details. Hoechst stain was used to mark the nuclei. Scale bars indicate 50 μm in **(A)** and **(B)**, and 100 μm in **(C)**. Act, activin A; BMP, bone morphogenetic factor; Bra, brachyury; Chi, chiron CHIR99021; E-Cad, E-cadherin; LB, leukaemia inhibitory factor and bone morphogenetic factor; LIF, leukaemia inhibitory factor.

Additional file 3: Figure S3. Pearson correlation coefficients. Values for Nanog and Oct4 (top), Nanog and Sox2 (bottom) for the different time points for Act, Chi and Act/Chi. The horizontal line represents the correlation for LB. Differentiation produces strong correlations between Nanog and Oct4 conditions whereas the correlation between Nanog and Sox2 increases with time. AC, activin A + chiron; Act, activin A; Chi, chiron CHIR99021; LB, leukaemia inhibitory factor and bone morphogenetic factor.

Additional file 4: Figure S4. Wnt/β-catenin transcriptional reporter (TLC2) following mesodermal differentiation. **(A)** Still images from live imaging of Bra::GFP mESCs in Act/Chi conditions (Additional file 5: Movie M1) showing phase contrast (top rows) and fluorescence (bottom rows). Act treatment results in lower levels of fluorescence compared with Chi or Act/Chi (Figure 4). **(B)** The number of cells tracked per condition over time. **(C)** The mean square displacement (MSD) of individual cells. Cell traces were separated into 10-h time intervals based on the time of tracking initiation. The number of cells within each time interval is displayed. The start of each cell trace within each time interval is aligned. See text for details. **(D)** Distribution of turning angles for all cells treated with Act, Chi and Act/Chi. A serum-LIF control from the TLC2 reporter cell line is included for comparison. There appears to be no bias in the direction cells move with respect to the conditions in which they are placed. **(E)** TLC2 reporter cells fixed at the indicated times and stained for Bra. Scale bar in all images denotes 50 μm. AC, activin A + chiron; Act, activin A; BMP, bone morphogenetic factor; Bra, brachyury; Chi, chiron CHIR99021; SL, serum leukaemia inhibitory factor; MSD, mean-squared displacement.

Additional file 5: Movie M1. Live imaging of Bra::GFP cells cultured in Act/Chi. Bra::GFP mESCs were plated in N2B27 supplemented with Act/Chi. As time progresses, cells begin to display EMT-like movements, become openly motile and begin to express Bra::GFP. Time in h.

Additional file 6: Movie M2. Live imaging of the β-catenin transcriptional reporter line (TLC2) following treatment with Act/Chi. The TCF/LEF::mCherry (TLC2) mESC reporter line was plated in N2B27 supplemented with Act/Chi. Cells initially expressed low and heterogeneous levels of the reporter, which increased over time in the cells that would eventually undergo an EMT event and disperse from the colony. Following colony exit, cells began to down-regulate the reporter. Time in hours.

Additional file 7: Figure S5. An EMT event is required for brachyury expression. **(A,B)** E14-Tg2A mESCs treated with Act **(A)** or Act/Chi **(B)** in the presence of CsA (3 μM) or DMSO for 48 and 96 h and stained for Hoechst, E-cadherin, β-catenin and Bra. In the presence of CsA, E-cadherin is not effectively cleared from the membrane, β-catenin does not enter the nucleus and there is no effective expression of Bra. **(C)** Stills from live imaging of E14-Tg2A mESCs in Act with DMSO or CsA. As with Chi (Figure 5C) cells in CsA stretch out filopodia but do not undergo an EMT. **(D)** The number of cells tracked in each condition over time. Scale bar in all images denote 50 μm. AC, activin A + chiron; Act, activin A; β-cat, β-catenin; Bra, brachyury; Chi, chiron CHIR99021; CsA, cyclosporine A; DMSO, dimethyl sulfoxide; E-Cad, E-cadherin; EMT, epithelial-to-mesenchymal transition; mESC, mouse embryonic stem cell.

Additional file 8: Figure S6. Immunofluorescence analysis and live-cell imaging of Nanog-/- mESCs following differentiation. **(A)** The number of cells tracked in each condition over time for WT, Nanog$^{-/-}$ and β-catenin$^{-/-}$ mESCs. **(B)** Time evolution of the distributions of the expression of Bra in Nanog$^{-/-}$ mESCs. The cells, treated with Act/Chi for 24, 48 and 72 h, were stained for Bra and nuclei were segmented based on Hoechst staining. The average pixel intensity for each fluorescent channel was quantified and the intensity of Bra displayed as histograms for each time point. The bisecting orange lines in each histogram correspond to the mean fluorescence levels. **(C)** Live imaging of Nanog mutants in Act/Chi. **(D)** Individual cell velocities (μm/h), and the average velocity profile for each cell line (indicated by colours) in Act/Chi. **(E)** The distribution of velocities over time. For comparison, the velocities and distribution of velocities for the WT and β-catenin mutant cell lines (Figure 6) are included in **(D)** and **(E)**. AC, activin A + chiron; Act, activin A; AFU, arbitrary fluorescence units; Bra, brachyury; Chi, chiron CHIR99021; mESC, mouse embryonic stem cell; Vel., velocity; WT, wild type.

Additional file 9: Figure S7. Analysis of individual Bra-/- cells from live-imaging experiments following Act, Chi and Act/Chi stimulation. **(A)** The number Bra$^{-/-}$ mESCs tracked from live-cell imaging (Figure 7) in each condition over time. **(B)** The mean square displacement (MSD) of individual cells. Cell traces were separated into 10-h time intervals based on the time of tracking initiation. The number of cells within each time interval is displayed. The start of each cell trace within each time interval is aligned. See text for details. AC, activin A + chiron; Act, activin A; Bra, brachyury; Chi, chiron CHIR99021; mESC, mouse embryonic stem cell; MSD, mean-squared displacement.

Additional file 10: Table S1. Summary of the tracking data. For each cell line used in the live-cell imaging experiments within this investigation (leftmost column: cell type), the number of movies analysed, the temporal resolution (frames/h), spatial resolution (pixels/μm), the number of cells tracked, positions tracked and the average number of positions per cell for each medium condition (second column from the left; medium conditions) to which the cells were exposed was tabulated. The total number of movies analysed and the total number of cells tracked throughout the investigation are recorded at the bottom of the table. This table can be used in conjunction with the number of cells tracked over time, displayed in Additional file 4: Figure S4B, Additional file 7: Figure S5D, Additional file 8: Figure S6A and Additional file 9: Figure S7A.

Abbreviations

AC: activin A + chiron; Act: activin A; AFU: arbitrary fluorescence units; BMP: bone morphogenetic factor; Bra: brachyury; Chi: chiron CHIR99021; CsA: cyclosporine A; DMSO: dimethyl sulfoxide; ECM: extracellular matrix; EMT: epithelial-to-mesenchymal transition; ESC: embryonic stem cell; ESLIF: medium containing serum and LIF; FACS: fluorescence-activated cell sorting; GAPDH: glyceraldehyde 3-phosphate dehydrogenase; GFP: green fluorescent protein; LB: leukaemia inhibitory factor and bone morphogenetic factor; LIF: leukaemia inhibitory factor; mESC: mouse embryonic stem cell; MSD: mean-squared displacement; QIA: quantitative image analysis; RFP: red fluorescent protein; RT-qPCR: quantitative real-time reverse-transcription-polymerase chain reaction; SB43: nodal/Act receptor inhibitor SB431542.

Competing interests

The authors declare that they have no competing interests.

Authors' contributions

AMA and DAT outlined the project and the experiments. DAT performed the experiments and analysed the data. JPM and PR developed the software for the analysis of the data. DAT, PR, JPM and ED analysed the data. DAT and AMA wrote the manuscript. All authors approved the final manuscript.

Acknowledgements

We thank F Bonkhofer for assistance with qRT-PCR, Drs A K Hadjantonakis, P Hayward, PF Machado, S Muñoz-Descalzo and C Schröter and the AMA lab for comments and discussions, Daniel Martinez Gatell for assistance in the manual tracking of cells, Carl Zeiss for technical support, G Keller for providing the Bra::GFP line, K Hadjantonakis for the TCF/LEF-mCherry cell line and V Wilson for the Bra mutant cell line. This research is funded by an ERC advanced grant to AMA. This article was previously made available on the BioRxiv preprint server [92].

Received: 16 May 2014 Accepted: 25 July 2014
Published online: 13 August 2014

References

1. Wolpert L, Tickle C: *Principles of Development*. New York, USA: Oxford University Press; 2010.
2. Martinez Arias A, Stewart A: *Molecular Principles of Animal Development*. Oxford, UK: Oxford University Press; 2002.
3. Gilbert SF: *Developmental Biology*. Sunderland, Massachusetts, USA: Sinauer Associates Inc.; 2013.
4. Ramkumar N, Anderson KV: **SnapShot: mouse primitive streak.** *Cell* 2011, **146:**488.
5. Solnica-Krezel L, Sepich DS: **Gastrulation: making and shaping germ layers.** *Annu Rev Cell Dev Biol* 2012, **28:**687–717.
6. Tam PPL, Gad JM: **Gastrulation in the mouse embryo**. In *Gastrulation: From Cells to Embryo*. 1st edition. Edited by Stern CD. New York: Cold Spring Harbor Laboratory Press; 2004:731.
7. Nowotschin S, Hadjantonakis A-K: **Cellular dynamics in the early mouse embryo: from axis formation to gastrulation.** *Curr Opin Genet Dev* 2010, **20:**420–427.
8. Fehling HJ, Lacaud G, Kubo A, Kennedy M, Robertson S, Keller G, Kouskoff V: **Tracking mesoderm induction and its specification to the hemangioblast during embryonic stem cell differentiation.** *Development* 2003, **130:**4217–4227.
9. Rivera-Pérez JA, Magnuson T: **Primitive streak formation in mice is preceded by localized activation of brachyury and Wnt3.** *Dev Biol* 2005, **288:**363–371.
10. Beddington RS, Rashbass P, Wilson V: **Brachyury – a gene affecting mouse gastrulation and early organogenesis.** *Dev Suppl* 1992, **166:**157–165.
11. Wilkinson DG, Bhatt S, Herrmann BG: **Expression pattern of the mouse T gene and its role in mesoderm formation.** *Nature* 1990, **343:**657–659.
12. Arnold SJ, Robertson EJ: **Making a commitment: cell lineage allocation and axis patterning in the early mouse embryo.** *Nat Rev Mol Cell Biol* 2009, **10:**91–103.
13. Lim J, Thiery JP: **Epithelial-mesenchymal transitions: insights from development.** *Development* 2012, **139:**3471–3486.
14. Thiery JP, Sleeman JP: **Complex networks orchestrate epithelial–mesenchymal transitions.** *Nat Rev Mol Cell Biol* 2006, **7:**131–142.
15. Williams M, Burdsal C, Periasamy A, Lewandoski M, Sutherland A: **Mouse primitive streak forms *in situ* by initiation of epithelial to mesenchymal transition without migration of a cell population.** *Dev Dyn* 2011, **241:**270–283.
16. Russ AP, Wattler S, Colledge WH, Aparicio S, Carlton MBL, Pearce JJ, Barton SC, Surani MA, Ryan K, Nehls MC: **Eomesodermin is required for mouse trophoblast development and mesoderm formation.** *Nature* 2000, **404:**95–98.
17. Robb L, Hartley L, Begley CG, Brodnicki TC, Copeland NG, Gilbert DJ, Jenkins NA, Elefanty AG: **Cloning, expression analysis, and chromosomal localization of murine and human homologues of a *Xenopus* mix gene.** *Dev Dyn* 2000, **219:**497–504.
18. Beddington RS: **Induction of a second neural axis by the mouse node.** *Development* 1994, **120:**613–620.
19. Smith JC: **Role of T-box genes during gastrulation**. In *Gastrulation: From Cells to Embryo*. 1st edition. Edited by Stern CD. New York: Cold Spring Harbor Laboratory Press; 2004:731.
20. Wilson V, Rashbass P, Beddington RS: **Chimeric analysis of T (brachyury) gene function.** *Development* 1993, **117:**1321–1331.
21. Cambray N, Wilson V: **Two distinct sources for a population of maturing axial progenitors.** *Development* 2007, **134:**2829–2840.
22. Gluecksohn-Schoenheimer S: **The development of two tailless mutants in the house mouse.** *Genetics* 1938, **23:**573.
23. Wilson V, Manson L, Skarnes W: **The T gene is necessary for normal mesodermal morphogenetic cell movements during gastrulation.** *Development* 1995, **121:**877–886.
24. Martin BL, Kimelman D: **Regulation of canonical Wnt signaling by brachyury is essential for posterior mesoderm formation.** *Dev Cell* 2008, **15:**121–133.
25. Tam PPL, Loebel DAF: **Gene function in mouse embryogenesis: get set for gastrulation.** *Nat Rev Genet* 2007, **8:**368–381.
26. Ichikawa T, Nakazato K, Keller PJ, Kajiura-Kobayashi H, Stelzer EHK, Mochizuki A, Nonaka S: **Live imaging of whole mouse embryos during gastrulation: migration analyses of epiblast and mesodermal cells.** *PLoS One* 2013, **8:**e64506.
27. Evans MJ, Kaufman MH: **Establishment in culture of pluripotential cells from mouse embryos.** *Nature* 1981, **292:**154–156.
28. Martin GR: **Isolation of a pluripotent cell line from early mouse embryos cultured in medium conditioned by teratocarcinoma stem cells.** *Proc Natl Acad Sci* 1981, **78:**7634–7638.
29. Hansson M, Olesen DR, Peterslund JML, Engberg N, Kahn M, Winzi M, Klein T, Maddox-Hyttel P, Serup P: **A late requirement for Wnt and FGF signaling during activin-induced formation of foregut endoderm from mouse embryonic stem cells.** *Dev Biol* 2009, **330:**286–304.
30. Ying Q-L, Smith AG: **Defined conditions for neural commitment and differentiation.** *Meth Enzymol* 2003, **365:**327–341.
31. Ying Q-L, Nichols J, Chambers I, Smith A: **BMP induction of Id proteins suppresses differentiation and sustains embryonic stem cell self-renewal in collaboration with STAT3.** *Cell* 2003, **115:**281–292.
32. Ying Q-L, Wray J, Nichols J, Batlle-Morera L, Doble B, Woodgett J, Cohen P, Smith A: **The ground state of embryonic stem cell self-renewal.** *Nature* 2008, **453:**519–523.
33. Ying Q-L, Stavridis M, Griffiths D, Li M, Smith A: **Conversion of embryonic stem cells into neuroectodermal precursors in adherent monoculture.** *Nat Biotechnol* 2003, **21:**183–186.
34. Gadue P, Huber TL, Paddison PJ, Keller GM: **Wnt and TGF-beta signaling are required for the induction of an *in vitro* model of primitive streak formation using embryonic stem cells.** *Proc Natl Acad Sci* 2006, **103:**16806–16811.
35. Kubo A, Shinozaki K, Shannon JM, Kouskoff V, Kennedy M, Woo S, Fehling HJ, Keller G: **Development of definitive endoderm from embryonic stem cells in culture.** *Development* 2004, **131:**1651–1662.
36. Keller G: **Embryonic stem cell differentiation: emergence of a new era in biology and medicine.** *Genes Dev* 2005, **19:**1129–1155.
37. Dobrovolskaia-Zavadskaia N: **Sur la mortification spontanée de la queue chez la souris nouveau-née et sur l'existence d'un caractère (facteur) heriditaire "non-viable".** *Comptes Rendus des Séances de la Société de Biologie* 1927, **97:**114–116.
38. Rashbass P, Cooke LA, Herrmann BG, Beddington RS: **A cell autonomous function of brachyury in T/T embryonic stem cell chimaeras.** *Nature* 1991, **353:**348–351.
39. Nakaya Y, Sukowati EW, Wu Y, Sheng G: **RhoA and microtubule dynamics control cell-basement membrane interaction in EMT during gastrulation.** *Nature* 2008, **10:**765–775.
40. Malaguti M, Nistor PA, Blin G, Pegg A, Zhou X, Lowell S, Miller F: **Bone morphogenic protein signalling suppresses differentiation of pluripotent cells by maintaining expression of E-cadherin.** *Elife* 2013, **2:**e01197.
41. Soncin F, Mohamet L, Eckardt D, Ritson S, Eastham AM, Bobola N, Russell A, Davies S, Kemler R, Merry CLR: **Abrogation of E-cadherin-mediated cell–cell contact in mouse embryonic stem cells results in reversible LIF-independent self-renewal.** *Stem Cells* 2009, **27:**2069–2080.
42. Chou Y-F, Chen H-H, Eijpe M, Yabuuchi A, Chenoweth JG, Tesar P, Lu J, McKay RDG, Geijsen N: **The growth factor environment defines distinct pluripotent ground states in novel blastocyst-derived stem cells.** *Cell* 2008, **135:**449–461.
43. Migeotte I, Grego-Bessa J, Anderson KV: **Rac1 mediates morphogenetic responses to intercellular signals in the gastrulating mouse embryo.** *Development* 2011, **138:**3011–3020.
44. Nakaya Y, Sheng G: **Epithelial to mesenchymal transition during gastrulation: an embryological view.** *Development Growth Diff* 2008, **50:**755–766.
45. Thomson M, Liu SJ, Zou L-N, Smith Z, Meissner A, Ramanathan S: **Pluripotency factors in embryonic stem cells regulate differentiation into germ layers.** *Cell* 2011, **145:**875–889.
46. Trott J, Arias AM: **Single cell lineage analysis of mouse embryonic stem cells at the exit from pluripotency.** *Biology Open* 2013, **2:**1049–1056.
47. Hart AH, Hartley L, Ibrahim M, Robb L: **Identification, cloning and expression analysis of the pluripotency promoting Nanog genes in mouse and human.** *Dev Dyn* 2004, **230:**187–198.
48. Chambers I, Silva J, Colby D, Nichols J, Nijmeijer B, Robertson M, Vrana J, Jones K, Grotewold L, Smith A: **Nanog safeguards pluripotency and mediates germline development.** *Nature* 2007, **450:**1230–1234.

49. Osorno R, Tsakiridis A, Wong F, Cambray N, Economou C, Wilkie R, Blin G, Scotting PJ, Chambers I, Wilson V: **The developmental dismantling of pluripotency is reversed by ectopic Oct4 expression.** *Development* 2012, **139:**2288–2298.
50. Arnold SJ, Stappert J, Bauer A, Kispert A, Herrmann BG, Kemler R: **Brachyury is a target gene of the Wnt/β-catenin signaling pathway.** *Mech Dev* 2000, **91:**249–258.
51. Yamaguchi TP, Takada S, Yoshikawa Y, Wu N, McMahon AP: **T (brachyury) is a direct target of Wnt3a during paraxial mesoderm specification.** *Genes Dev* 1999, **13:**3185–3190.
52. Faunes F, Hayward P, Descalzo SM, Chatterjee SS, Balayo T, Trott J, Christoforou A, Ferrer-Vaquer A, Hadjantonakis A-K, Dasgupta R, Arias AM: **A membrane-associated β-catenin/Oct4 complex correlates with ground-state pluripotency in mouse embryonic stem cells.** *Development* 2013, **140:**1171–1183.
53. Ferrer-Vaquer A, Piliszek A, Tian G, Aho RJ, Dufort D, Hadjantonakis A-K: **A sensitive and bright single-cell resolution live imaging reporter of Wnt/β-catenin signaling in the mouse.** *BMC Dev Biol* 2010, **10:**121.
54. Clipstone NA, Crabtree GR: **Identification of calcineurin as a key signalling enzyme in T-lymphocyte activation.** *Nature* 1992, **357:**695–697.
55. Li X, Zhu L, Yang A, Lin J, Tang F, Jin S, Wei Z, Li J, Jin Y: **Calcineurin-NFAT signaling critically regulates early lineage specification in mouse embryonic stem cells and embryos.** *Stem Cell* 2011, **8:**46–58.
56. Mancini M, Toker A: **NFAT proteins: emerging roles in cancer progression.** *Nat Rev Cancer* 2009, **9:**810–820.
57. Yilmaz M, Christofori G: **EMT, the cytoskeleton, and cancer cell invasion.** *Cancer Metastasis Rev* 2009, **28:**15–33.
58. Yu P, Pan G, Yu J, Thomson JA: **FGF2 sustains NANOG and switches the outcome of BMP4-induced human embryonic stem cell differentiation.** *Cell Stem Cell* 2011, **8:**326–334.
59. Zhu Z, Huangfu D: **Human pluripotent stem cells: an emerging model in developmental biology.** *Development* 2013, **140:**705–717.
60. Murry CE, Keller G: **Differentiation of embryonic stem cells to clinically relevant populations: lessons from embryonic development.** *Cell* 2008, **132:**661–680.
61. Wilson V, Beddington R: **Expression of T protein in the primitive streak is necessary and sufficient for posterior mesoderm movement and somite differentiation.** *Dev Biol* 1997, **192:**45–58.
62. Villegas SN, Rothová M, Barrios-Llerena ME, Pulina M, Hadjantonakis A-K, Le Bihan T, Astrof S, Brickman JM: **PI3K/Akt1 signalling specifies foregut precursors by generating regionalized extra-cellular matrix.** *Elife* 2013, **2:**e00806.
63. Cheng P, Andersen P, Hassel D, Kaynak BL, Limphong P, Juergensen L, Kwon C, Srivastava D: **Fibronectin mediates mesendodermal cell fate decisions.** *Development* 2013, **140:**2587–2596.
64. Snow M: **Gastrulation in the mouse: growth and regionalization of the epiblast.** *J Embryol Exp Morphol* 1977, **42:**293–303.
65. Tada M, Smith JC: **Xwnt11 is a target of *Xenopus* brachyury: regulation of gastrulation movements via dishevelled, but not through the canonical Wnt pathway.** *Development* 2000, **127:**2227–2238.
66. Hoffman JA, Wu C-I, Merrill BJ: **Tcf7l1 prepares epiblast cells in the gastrulating mouse embryo for lineage specification.** *Development* 2013, **140:**1665–1675.
67. Izumi N, Era T, Akimaru H, Yasunaga M, Nishikawa S-I: **Dissecting the molecular hierarchy for mesendoderm differentiation through a combination of embryonic stem cell culture and RNA interference.** *Stem Cells* 2007, **25:**1664–1674.
68. Gentsch GE, Owens NDL, Martin SR, Piccinelli P, Faial T, Trotter MWB, Gilchrist MJ, Smith JC: ***In vivo* T-box transcription factor profiling reveals joint regulation of embryonic neuromesodermal bipotency.** *Cell Rep* 2013, **4:**1185–1196.
69. Evans AL, Faial T, Gilchrist MJ, Down T, Vallier L, Pedersen RA, Wardle FC, Smith JC: **Genomic targets of brachyury (T) in differentiating mouse embryonic stem cells.** *PLoS One* 2012, **7:**e33346.
70. Shimoda M, Sugiura T, Imajyo I, Ishii K, Chigita S, Seki K, Kobayashi Y, Shirasuna K: **The T-box transcription factor brachyury regulates epithelial-mesenchymal transition in association with cancer stem-like cells in adenoid cystic carcinoma cells.** *BMC Cancer* 2012, **12:**377.
71. Hardy KM, Garriock RJ, Yatskievych TA, D'Agostino SL, Antin PB, Krieg PA: **Non-canonical Wnt signaling through Wnt5a/b and a novel Wnt11 gene, Wnt11b, regulates cell migration during avian gastrulation.** *Dev Biol* 2008, **320:**391–401.
72. Heisenberg CP, Tada M, Rauch G, Saude L: **Silberblick/Wnt 11 mediates convergent extension movements during zebrafish gastrulation.** *Nature* 2000, **405:**76–81.
73. Hashimoto K, Fujimoto H, Nakatsuji N: **An ECM substratum allows mouse mesodermal cells isolated from the primitive streak to exhibit motility similar to that inside the embryo and reveals a deficiency in the T/T mutant cells.** *Development* 1987, **100:**587–598.
74. Nakatsuji N, Snow MH, Wylie CC: **Cinemicrographic study of the cell movement in the primitive-streak-stage mouse embryo.** *J Embryol Exp Morphol* 1986, **96:**99–109.
75. Wittler L, Shin E-H, Grote P, Kispert A, Beckers A, Gossler A, Werber M, Herrmann BG: **Expression of Msgn1 in the presomitic mesoderm is controlled by synergism of WNT signalling and Tbx6.** *EMBO Rep* 2007, **8:**784–789.
76. Nowotschin S, Ferrer-Vaquer A, Concepcion D, Papaioannou VE, Hadjantonakis A-K: **Interaction of Wnt3a, Msgn1 and Tbx6 in neural versus paraxial mesoderm lineage commitment and paraxial mesoderm differentiation in the mouse embryo.** *Dev Biol* 2012, **367:**1–14.
77. Blanchard GB, Kabla AJ, Schultz NL, Butler LC, Sanson B, Gorfinkiel N, Mahadevan L, Adams RJ: **Tissue tectonics: morphogenetic strain rates, cell shape change and intercalation.** *Nat Chem Biol* 2009, **6:**458–464.
78. Slagle CE, Aoki T, Burdine RD: **Nodal-dependent mesendoderm specification requires the combinatorial activities of FoxH1 and eomesodermin.** *PLoS Genet* 2011, **7:**e1002072.
79. Teo AKK, Arnold SJ, Trotter MWB, Brown S, Ang LT, Chng Z, Robertson EJ, Dunn NR, Vallier L: **Pluripotency factors regulate definitive endoderm specification through eomesodermin.** *Genes Dev* 2011, **25:**238–250.
80. Arnold SJ, Hofmann UK, Bikoff EK, Robertson EJ: **Pivotal roles for eomesodermin during axis formation, epithelium-to-mesenchyme transition and endoderm specification in the mouse.** *Development* 2008, **135:**501–511.
81. Wray J, Kalkan T, Gomez-Lopez S, Eckardt D, Cook A, Kemler R, Smith A: **Inhibition of glycogen synthase kinase-3 alleviates Tcf3 repression of the pluripotency network and increases embryonic stem cell resistance to differentiation.** *Nat Cell Biol* 2011, **13:**838–845.
82. Huang S-MA, Mishina YM, Liu S, Cheung A, Stegmeier F, Michaud GA, Charlat O, Wiellette E, Zhang Y, Wiessner S, Hild M, Shi X, Wilson CJ, Mickanin C, Myer V, Fazal A, Tomlinson R, Serluca F, Shao W, Cheng H, Shultz M, Rau C, Schirle M, Schlegl J, Ghidelli S, Fawell S, Lu C, Curtis D, Kirschner MW, Lengauer C, *et al*: **Tankyrase inhibition stabilizes axin and antagonizes Wnt signalling.** *Nature* 2009, **461:**614–620.
83. Chen B, Dodge ME, Tang W, Lu J, Ma Z, Fan C-W, Wei S, Hao W, Kilgore J, Williams NS, Roth MG, Amatruda JF, Chen C, Lum L: **Small molecule–mediated disruption of Wnt-dependent signaling in tissue regeneration and cancer.** *Nat Chem Biol* 2009, **5:**100–107.
84. Inman GJ, Nicolás FJ, Callahan JF, Harling JD, Gaster LM, Reith AD, Laping NJ, Hill CS: **SB-431542 is a potent and specific inhibitor of transforming growth factor-β superfamily type I activin receptor-like kinase (ALK) receptors ALK4, ALK5, and ALK7.** *Mol Pharmacol* 2002, **62:**65–74.
85. Yu PB, Hong CC, Sachidanandan C, Babitt JL, Deng DY, Hoyng SA, Lin HY, Bloch KD, Peterson RT: **Dorsomorphin inhibits BMP signals required for embryogenesis and iron metabolism.** *Nat Chem Biol* 2007, **4:**33–41.
86. Descalzo SM, Rué P, Garcia-Ojalvo J, Arias AM: **Correlations between the levels of Oct4 and Nanog as a signature for naïve pluripotency in mouse ES cells.** *Stem Cells* 2012, **30:**2683–2691.
87. Schindelin J, Arganda-Carreras I, Frise E, Kaynig V, Longair M, Pietzsch T, Preibisch S, Rueden C, Saalfeld S, Schmid B: **Fiji: an open-source platform for biological-image analysis.** *Nat Meth* 2012, **9:**676–682.
88. Meijering E, Dzyubachyk O, Smal I: **Methods for cell and particle tracking.** *Meth Enzymol* 2012, **504:**183–200.
89. Sage D, Unser M, Salmon P, Dibner C: **A software solution for recording circadian oscillator features in time-lapse live cell microscopy.** *Cell Division* 2010, **5:**17.

90. Dibner C, Sage D, Unser M, Bauer C, D'Eysmond T, Naef F, Schibler U: **Circadian gene expression is resilient to large fluctuations in overall transcription rates.** *EMBO J* 2009, **28:**123–134.
91. Boggy GJ, Woolf PJ: **A mechanistic model of PCR for accurate quantification of quantitative PCR data.** *PLoS One* 2010, **5:**e12355.
92. **Previous version of this article on the BioRxiv preprint server.** [http://dx.doi.org/10.1101/003871]

doi:10.1186/s12915-014-0063-7
Cite this article as: Turner *et al.*: Brachyury cooperates with Wnt/β-catenin signalling to elicit primitive-streak-like behaviour in differentiating mouse embryonic stem cells. *BMC Biology* 2014 **12**:63.

Submit your next manuscript to BioMed Central and take full advantage of:

- **Convenient online submission**
- **Thorough peer review**
- **No space constraints or color figure charges**
- **Immediate publication on acceptance**
- **Inclusion in PubMed, CAS, Scopus and Google Scholar**
- **Research which is freely available for redistribution**

Submit your manuscript at
www.biomedcentral.com/submit

BioMed Central